

Water Use in the Development and Operation of Geothermal Power Plants

Environmental Science Division

About Argonne National Laboratory

Argonne is a U.S. Department of Energy laboratory managed by UChicago Argonne, LLC under contract DE-AC02-06CH11357. The Laboratory's main facility is outside Chicago, at 9700 South Cass Avenue, Argonne, Illinois 60439. For information about Argonne and its pioneering science and technology programs, see www.anl.gov.

Availability of This Report

This report is available, at no cost, at <http://www.osti.gov/bridge>. It is also available on paper to the U.S. Department of Energy and its contractors, for a processing fee, from:

U.S. Department of Energy

Office of Scientific and Technical Information

P.O. Box 62

Oak Ridge, TN 37831-0062

phone (865) 576-8401

fax (865) 576-5728

reports@adonis.osti.gov

Disclaimer

This report was prepared as an account of work sponsored by an agency of the United States Government. Neither the United States Government nor any agency thereof, nor UChicago Argonne, LLC, nor any of their employees or officers, makes any warranty, express or implied, or assumes any legal liability or responsibility for the accuracy, completeness, or usefulness of any information, apparatus, product, or process disclosed, or represents that its use would not infringe privately owned rights. Reference herein to any specific commercial product, process, or service by trade name, trademark, manufacturer, or otherwise, does not necessarily constitute or imply its endorsement, recommendation, or favoring by the United States Government or any agency thereof. The views and opinions of document authors expressed herein do not necessarily state or reflect those of the United States Government or any agency thereof, Argonne National Laboratory, or UChicago Argonne, LLC.

Water Use in the Development and Operation of Geothermal Power Plants

by

C.E. Clark¹, C.B. Harto¹, J.L. Sullivan², and M.Q. Wang²

¹Environmental Science Division

²Energy Systems Division, Argonne National Laboratory

January 2011

CONTENTS

| | |
|---|------|
| ACKNOWLEDGMENTS | viii |
| ACRONYMS USED IN THIS DOCUMENT..... | ix |
| EXECUTIVE SUMMARY | 1 |
| 1 INTRODUCTION | 3 |
| 1.1 Purpose | 3 |
| 1.2 Overview of Study | 3 |
| 2 GEOTHERMAL ELECTRICITY GENERATION | 5 |
| 2.1 Conventional Hydrothermal Flash System | 5 |
| 2.2 Conventional Hydrothermal Binary System | 5 |
| 2.3 Enhanced Geothermal System | 5 |
| 2.4 Water and Geothermal Electricity Generation | 6 |
| 3 APPROACH AND METHODS | 7 |
| 3.1 Life Cycle Analysis | 7 |
| 3.2 Scenarios | 7 |
| 3.3 Well Field Development | 8 |
| 3.3.1 Well Construction | 9 |
| 3.3.2 Hydraulic Stimulation of the Resource | 10 |
| 3.4 Pipeline and Plant Construction | 11 |
| 3.4.1 Pipeline Supports..... | 12 |
| 3.4.2 Power Plant Construction..... | 12 |
| 3.5 Operations | 13 |
| 3.5.1 Makeup Water | 14 |
| 3.5.2 Cooling Water | 14 |
| 3.6 Water Quality | 16 |
| 4 RESULTS OF THE LIFE CYCLE ANALYSIS | 19 |
| 4.1 Construction and Stimulation..... | 19 |
| 4.2 Plant Operations and the Life Cycle | 21 |
| 4.3 Comparison with Other Power Plant Types | 25 |
| 5 ANALYSIS AND INTERPRETATION OF WATER QUALITY | 29 |
| 5.1 Geothermal Brine Characteristics | 29 |

CONTENTS (CONT.)

| | | |
|-----|--|----|
| 5.2 | Water pollution potential..... | 31 |
| 5.3 | Noncondensable Gases | 36 |
| 5.4 | Scale Formation and Corrosion..... | 41 |
| 5.5 | Mineral Extraction..... | 44 |
| 6 | SUMMARY AND CONCLUSIONS | 49 |
| 7 | REFERENCES | 51 |
| | APPENDIX A – ARGONNE GEOTHERMAL GEOCHEMICAL DATABASE | 57 |
| | APPENDIX B – DETAILED LIFE CYCLE INVENTORY DATA | 59 |
| | APPENDIX C – ADDITIONAL GEOCHEMICAL COMPOSITION DATA..... | 63 |
| | APPENDIX D – ADDITIONAL GAS COMPOSITION DATA | 69 |

FIGURES

| | | |
|-----|---|----|
| 3-1 | System Boundary for Well Field..... | 9 |
| 3-2 | Percent of U.S. Geothermal Power Production Capacity in 2007 by Technology | 15 |
| 3-3 | Percent of Total U.S. Geothermal Power Generating Units by Technology | 15 |
| 4-1 | Volume of Water Consumed for Construction of Geothermal Power Plants according to Scenarios and Assuming Average Depth for Wells | 20 |
| 4-2 | Water Consumption in Millions of Gallons per Megawatt as a Function of Well Depth for the Construction Stage of the EGS Scenarios | 21 |
| 4-3 | Water Volume in Millions of Gallons per Megawatt Consumed for the EGS Scenarios According to Depth | 22 |
| 4-4 | Contribution to Total Water Requirements by Process..... | 22 |
| 4-5 | Life Cycle Volume of Water Consumption in Millions of Gallons for Geothermal Power Plant Scenarios | 23 |
| 4-6 | Contribution of Operations Water Use to Total Water Use in the Power Plant Life Cycle | 23 |
| 4-7 | Water Consumption for Electric Power Generation | 28 |
| 5-1 | Distribution of pH Measurements for U.S. Geothermal Sources with Temperature Greater than 90°C | 30 |

FIGURES (CONT.)

| | |
|---|----|
| 5-2 Distribution of TDS Measurements for U.S. Geothermal Sources with Temperature Greater than 90°C | 30 |
| 5-3 Geofluid Composition Box Plots, Major Constituents..... | 32 |
| 5-4 Geofluid Composition Box Plots, Minor Constituents | 33 |
| 5-5 Geofluid Compositions of Selected Samples | 34 |
| 5-6 Histogram of Carbon Dioxide Concentrations in NCG Stream | 37 |
| 5-7 Histogram of Nitrogen Concentrations in NCG Stream | 38 |
| 5-8 Histogram of Combined Nitrogen and Carbon Dioxide Concentrations in NCG Stream | 38 |
| 5-9 Examples of Noncondensable Gas Composition..... | 40 |
| C-1 Geofluid Composition, Sample from Mesa 6-2 Well in CA at 187°C..... | 65 |
| C-2 Geofluid Composition, Sample from Mesa 31-1 Well in CA at 157°C..... | 65 |
| C-3 Geofluid Composition, Sample from Well 73b-7 in NV at 174°C | 66 |
| C-4 Geofluid Composition, Sample from Well 37-33 in NV at 165°C | 66 |
| C-5 Geofluid Composition, Sample from the 101 Separator in NV at 160°C | 67 |
| C-6 Geofluid Composition, Sample from Magma Power Co, Unspecified Well in CA at 94°C | 67 |
| C-7 Geofluid Composition, Sample from Breitenbush Hot Springs, in OR at 92°C..... | 68 |
| C-8 Geofluid Composition, Sample from an Unnamed Spring in CA at 90°C..... | 68 |
| D-1 NCG Composition, Sample from Steamboat Hills in NV at 154°C | 69 |
| D-2 NCG Composition, Sample from Crump Geyser in OR at 99°C..... | 69 |
| D-3 NCG Composition, Sample from Leach Hot Spring in NV at 97°C..... | 70 |
| D-4 NCG Composition, Sample from Sapphire Geyser in WY at 95°C..... | 70 |

FIGURES (CONT.)

| | |
|--|----|
| D-5 NCG Composition, Sample from Casa Diablo in CA at 93°C..... | 71 |
| D-6 NCG Composition, Sample from Amadee Hot Springs in CA at 92°C..... | 71 |
| D-7 NCG Composition, Sample from Shoshone Basin in WY at 92°C..... | 72 |
| D-8 NCG Composition, Sample from Thermo Hot Springs in UT at 89°C..... | 72 |
| D-9 NCG Composition, Sample from Worswick Hot Springs in ID at 86°C..... | 73 |
| D-10 NCG Composition, Sample from Port Moller Hot Springs in AK at 71°C..... | 73 |
| D-11 NCG Composition, Sample from Travertine Hot Springs in CA at 69°C..... | 74 |

TABLES

| | |
|--|----|
| 3-1 Parameter Values for Four Geothermal Power Plant Scenarios..... | 8 |
| 3-2 Water Volume Requirements by Step for Stimulation Process of One Well..... | 11 |
| 3-3 Material Requirements for Concrete Mix for Foundation Supports for a 1,000-m Pipeline | 12 |
| 3-4 Material and Water Requirements for Geothermal Power Plant Construction..... | 13 |
| 3-5 Average Flow Rates for Four Geothermal Scenarios..... | 13 |
| 3-6 Average Flow Rates from Historical Production and Injection Data for Several California Geothermal Power Plants | 14 |
| 3-7 Geofluid Chemical Composition Data Sources..... | 17 |
| 4-1 Average Number of Wells by Scenario..... | 19 |
| 4-2 Average Water Consumption Estimates for Geothermal Power Generation by Life Cycle Stage over Plant Lifetime in Gallons per kWh of Lifetime Energy Output..... | 24 |
| 4-3 Aggregated Water Consumption for Electric Power Generation at Indicated Life Cycle Stages in Gallons Per kWh of Lifetime Energy Output | 26 |

TABLES (CONT.)

| | |
|---|----|
| 5-1 Comparison of Geofluid Composition with U.S. Primary Drinking Water Standards | 35 |
| 5-2 Comparison of Geofluid Composition with U.S. Secondary Drinking Water Standards | 35 |
| 5-3 Summary of Geothermal Scale Formation Mechanisms and Mitigation Options | 43 |
| 5-4 Summary of Known Geothermal Byproduct Recovery Projects | 45 |
| 5-5 Analysis of Potential Revenue from Mineral Extraction at the East Mesa, CA, Geothermal Field | 47 |
| 5-6 Comparison of Economic Potential from Mineral Extraction of a Range of Geothermal Wells..... | 47 |
| B-1 Water Use by Life Cycle Stage. | 59 |
| B-2 Water Consumption where Significant for Electric Power Generation at Indicated Life Cycle Stages — in Gallons Per kWh of Lifetime Energy Output | 60 |
| C-1 Summary of Geofluid Constituent Concentrations for Different Temperature Ranges..... | 63 |

ACKNOWLEDGMENTS

Argonne National Laboratory's work was supported by the U.S. Department of Energy, Assistant Secretary for Energy Efficiency and Renewable Energy, Office of Geothermal Technologies, under contract DE-AC02-06CH11357. The authors acknowledge and are grateful for the expert assistance of Gregory Mines, Idaho National Laboratory; A.J. Mansure, Geothermal Consultant; and Michael McLamore, Argonne National Laboratory, in our data-gathering and modeling efforts. We also thank our sponsor, Arlene Anderson of the Office of Geothermal Technologies, Office of Energy Efficiency and Renewable Energy, U.S. Department of Energy.

ACRONYMS USED IN THIS DOCUMENT

| | |
|-------|--|
| AGGD | Argonne Geothermal Geochemical Database |
| API | American Petroleum Institute |
| CSP | concentrated solar power |
| DOE | U.S. Department of Energy |
| EGS | enhanced geothermal systems |
| EIA | Energy Information Administration |
| EPRI | Electric Power Research Institute |
| GBGGD | Great Basin Groundwater Geochemical Database |
| GETEM | Geothermal Electricity Technology Evaluation Model |
| GHG | greenhouse gas |
| IGCC | integrated gasification combined cycle |
| LCA | life cycle analysis |
| MCL | maximum contaminant level |
| MWe | megawatts of electricity produced |
| NCG | noncondensable gases |
| NETL | National Energy Technology Laboratory |
| NGCC | natural gas combined cycle |
| PV | photovoltaics |
| TDS | total dissolved solids |

WATER USE IN THE DEVELOPMENT AND OPERATION OF GEOTHERMAL POWER PLANTS

C.E. Clark, C.B. Harto, J.L. Sullivan, and M.Q. Wang

EXECUTIVE SUMMARY

Geothermal energy is increasingly recognized for its potential to reduce carbon emissions and U.S. dependence on foreign oil. Energy and environmental analyses are critical to developing a robust set of geothermal energy technologies. This report summarizes what is currently known about the life cycle water requirements of geothermal electric power-generating systems and the water quality of geothermal waters. It is part of a larger effort to compare the life cycle impacts of large-scale geothermal electricity generation with other power generation technologies. The results of the life cycle analysis are summarized in a companion report, *Life Cycle Analysis Results of Geothermal Systems in Comparison to Other Power Systems*.

This report is divided into six chapters. Chapter 1 gives the background of the project and its purpose, which is to inform power plant design and operations. Chapter 2 summarizes the geothermal electricity generation technologies evaluated in this study, which include conventional hydrothermal flash and binary systems, as well as enhanced geothermal systems (EGS) that rely on engineering a productive reservoir where heat exists but water availability or permeability may be limited.

Chapter 3 describes the methods and approach to this work and identifies the four power plant scenarios evaluated: a 20-MW EGS plant, a 50-MW EGS plant, a 10-MW binary plant, and a 50-MW flash plant. The two EGS scenarios include hydraulic stimulation activities within the construction stage of the life cycle and assume binary power generation during operations. The EGS and binary scenarios are assumed to be air-cooled power plants, whereas the flash plant is assumed to rely on evaporative cooling. The well field and power plant design for the scenario were based on simulations using DOE's Geothermal Economic Technology Evaluation Model (GETEM).

Chapter 4 presents the water requirements for the power plant life cycle for the scenarios evaluated. Geology, reservoir characteristics, and local climate have various effects on elements such as drilling rate, the number of production wells, and production flow rates. Over the life cycle of a geothermal power plant, from construction through 30 years of operation, plant operations is where the vast majority of water consumption occurs. Water consumption refers to the water that is withdrawn from a resource such as a river, lake, or non-geothermal aquifer that is not returned to that resource. For the EGS scenarios, plant operations consume between 0.29 and 0.72 gal/kWh. The binary plant experiences similar operational consumption, at 0.27 gal/kWh. Far less water, just 0.01 gal/kWh, is consumed during operations of the flash plant because geofluid is used for cooling and is not replaced.

While the makeup water requirements are far less for a hydrothermal flash plant, the long-term sustainability of the reservoir is less certain due to estimated evaporative losses of

14.5–33% of produced geofluid at operating flash plants. For the hydrothermal flash scenario, the average loss of geofluid due to evaporation, drift, and blowdown is 2.7 gal/kWh.

The construction stage requires considerably less water: 0.001 gal/kWh for both the binary and flash plant scenarios and 0.01 gal/kWh for the EGS scenarios. The additional water requirements for the EGS scenarios are caused by a combination of factors, including lower flow rates per well, which increases the total number of wells needed per plant, the assumed well depths, and the hydraulic stimulation required to engineer the reservoir.

Water quality results are presented in Chapter 5. The chemical composition of geofluid has important implications for plant operations and the potential environmental impacts of geothermal energy production. An extensive dataset containing more than 53,000 geothermal geochemical data points was compiled and analyzed for general trends and statistics for typical geofluids. Geofluid composition was found to vary significantly both among and within geothermal fields. Seven main chemical constituents were found to account for 95–99% of the dissolved solids in typical geofluids. In order of abundance, they were chloride, sodium, bicarbonate, sulfate, silica, calcium, and potassium.

The potential for water and soil contamination from accidents and spills was analyzed by comparing geofluid composition with U.S. drinking water standards. Geofluids were found to present a potential risk to drinking water, if released, due to high concentrations of antimony, arsenic, lead, and mercury. That risk could be mitigated through proper design and engineering controls.

The concentration and impact of noncondensable gases (NCG) dissolved in the geofluid was evaluated. The majority of NCG was either nitrogen or carbon dioxide, but a small number of geofluids contain potentially recoverable concentrations of hydrogen or methane. The main drivers for scale and corrosion were identified and their potential operational impact and key mitigation strategies were discussed. Finally, the potential for mineral extraction from the geofluid was evaluated and it was concluded that while the value of minerals contained within some geofluids can be very high in some cases, historically the economics of extraction have proved to be quite challenging.

While air-cooled systems do not require water for cooling, operational water losses do occur in practice. The life cycle analysis reveals that the consumptive losses aggregated over 30 years are significant to the overall water requirements for geothermal power plant systems, suggesting that efforts to reduce water consumption should focus on identifying these losses and exploring opportunities for water efficiency improvements. Although flash plant operations appear to be more water efficient, the long-term sustainability of the reservoir is uncertain. In general, binary systems were found to help mitigate some of the operational and environmental concerns related to geofluids, by eliminating any gas venting to the atmosphere, reducing the carbon footprint and the need for hydrogen sulfide controls, and minimizing or eliminating some of the key drivers of scale formation.

1 INTRODUCTION

Increasing concerns over climate change and a desire to reduce U.S. dependence on foreign oil have renewed the national interest in alternative energy resources. The Energy Information Administration (EIA) of the U.S. Department of Energy (DOE) projects that renewable electricity, which now represents around 8.5% of U.S. electricity generation, will increase to about 17% by 2035 (EIA, 2010).

While most of the increase in renewable electricity is projected to come from wind turbines and biomass combustion plants, geothermal electricity generation is projected to increase 60% during the same time frame. Geothermal power, customarily associated with states with conspicuous geothermal resources (e.g., geysers or fumaroles), could grow even more if enhanced geothermal systems (EGS) technology, which can effectively operate on more broadly available lower-temperature geofluids, proves to be a good cost and environmental performer. Coupling this with the fact that geothermal plants tend to run trouble-free at or near full capacity for most of their lifetimes, geothermal power could become a viable option for many states and in the process become a significant contributor to the U.S. power infrastructure.

1.1 PURPOSE

This work is part of a larger project supporting the Geothermal Technologies Program of DOE's Office of Energy Efficiency and Renewable Energy that compares the energy and environmental impacts of EGS with conventional geothermal and other nongeothermal systems for electricity generation. Argonne National Laboratory carried out a life cycle analysis (LCA), reported in a companion document (Sullivan et al., 2010), to quantify energy and environmental benefits of EGS by examining proximity to infrastructure, resource availability, and tradeoffs associated with well depth and resource temperature. This report summarizes the LCA effort as it pertains to water use in geothermal power plants. A special emphasis is placed on the category of water required for each process in the life cycle.

The scope of this work is limited to the quantification of on-site water requirements. While materials for the construction of geothermal power plants have upstream water burdens embedded in industrial processes and energy consumption, their water impacts are not necessarily allocated to the watershed or aquifers associated with a power plant and are not included in this analysis.

1.2 OVERVIEW OF STUDY

With significant potential growth opportunities for geothermal technologies, it is important to understand the material and energy requirements for geothermal energy development and its potential environmental impacts. Life cycle energy and greenhouse gas emissions simulations were conducted for enhanced geothermal, hydrothermal flash, and

hydrothermal binary power-generating technologies for scenarios developed with input from subject matter experts. Argonne's GREET model was expanded to address life cycle emissions and energy issues so that reductions in fossil energy use, petroleum use, greenhouse gas (GHG) emissions, and criteria air pollutant emissions by EGS could be thoroughly examined by stakeholders. As the inventory for this analysis was conducted, water use associated with the process was also quantified. The results of the water inventory and an assessment of geofluid composition and its implications for water quality and system design are presented herein.

2 GEOTHERMAL ELECTRICITY GENERATION

Geothermal electricity generation has been possible since 1904 (Lund, 2004). The first type of geothermal power plant was a dry-steam plant, which relied upon a vapor-phase geofluid. Because large dry-steam reservoirs are rare and generally already developed (e.g., Larderello in Tuscany and The Geysers in California), the focus of this work is on hydrothermal systems. This chapter describes the different types of hydrothermal systems and water use patterns in geothermal electricity production.

2.1 CONVENTIONAL HYDROTHERMAL FLASH SYSTEM

Hydrothermal fluids above 182°C (360°F) can be used in flash plants to make electricity (USDOJ and USDA, 2008). For the purposes of this assessment, temperatures between 175°C and 300°C were considered. The geofluid is rapidly vaporized or “flashed,” either as it ascends from the well or at the plant, where the geofluid flows into a tank held at a much lower pressure. The vapor drives a turbine, which then drives a generator. Any liquid that remains in the tank can be flashed again in a second system to generate more electricity. The vapor from these systems is typically released to the atmosphere while the condensate is reinjected to an underground reservoir.

2.2 CONVENTIONAL HYDROTHERMAL BINARY SYSTEM

Energy can be extracted in binary-cycle power plants from geothermal reservoirs with moderate temperatures between 74°C and 182°C (USDOJ and USDA, 2008). Geofluid temperatures between 150°C and 185°C were considered for this LCA. In binary-cycle plants, geothermal fluid is pumped from a well and flows through a heat exchanger to warm a secondary fluid, which is often referred to as the “working fluid.” The working fluid has a much lower boiling point than the geofluid. The heat from the geofluid causes the working fluid to flash to vapor, which then drives a turbine. Because this is a closed-loop system, virtually nothing is emitted to the atmosphere. Moderate-temperature water is by far the more common geothermal resource; most geothermal power plants in the future will be binary-cycle plants.

2.3 ENHANCED GEOTHERMAL SYSTEM

EGS can expand the electricity-generating capacity of geothermal resources. By injecting water into the subsurface resource, existing fractures can be expanded or new fractures can be created to improve water circulation through the resource. These systems can be implemented in formations that are dryer and deeper than conventional geothermal resources (DOE, 2008a). Temperatures considered for this LCA were between 175°C and 225°C. Because of the increased depths and temperatures, and decreased water availability, of the resources involved, environmental impacts from EGS can be different from conventional geothermal power plants.

2.4 WATER AND GEOTHERMAL ELECTRICITY GENERATION

Water is required for both traditional geothermal systems and EGS throughout the life cycle of a power plant. For traditional projects, the water available at the resource is typically used for energy generation during plant operations. Depending on the technology employed for electricity generation, production can lower the water table over time, affecting surrounding areas (Tester et al., 2006; Lee, 2004). In addition to being used for energy generation, water is also used for cooling the working fluid in the plant. Wet cooling towers are used when makeup water from nearby surface waters or other water supplies are available. Air cooling is an effective alternative when water supplies are limited.

Water is used in EGS for drilling wells; constructing wells, pipelines, and plant infrastructure; stimulating the injection wells; and operating the power plant. Although water extracted from the formation is reinjected after use, some water is lost to the formation. To maintain pressure and operation, water that is lost must be made up from alternative water sources.

In addition to risk to water quantity, there may be some risk to water quality. During drilling and operations, additives may be used to reduce solid deposition on equipment and casings. Water produced from underground formations for geothermal electric power generation often exceeds primary and secondary drinking water standards for total dissolved solids, fluoride, chloride, and sulfate (USEPA, 1987, 1999). While the risk of aquifer contamination exists for both conventional geothermal systems and EGS, dissolved solids increase significantly with an increase in temperature, increasing the magnitude of contamination should a leak occur within an EGS. According to White et al. (1971), water from high-temperature formations are nearly always characterized by relatively high amounts of chlorides, silica, boron, and arsenic.

For conventional geothermal systems, care in site selection can mitigate much of the risk to nearby aquifers. Additionally, solids can be collected and removed; with proper management, surface impacts from waste generation can be minimized. The risk of aquifer contamination for EGS can be mitigated through redundancy in well design. Surface contamination is mitigated through reinjection of produced fluid, although solids collection or chemical treatment may still be required to address precipitation of dissolved solids after heat transfer.

3 APPROACH AND METHODS

To improve understanding of the potential environmental impacts of geothermal electricity generation, an LCA was conducted to account for energy, emissions, materials, and water requirements. This report covers the water requirements portion of the analysis. In addition to quantifying the amount of water required for geothermal electricity generation, a goal of this work is to profile the water quality of the geofluid. The results will inform design considerations for power plants and suggest opportunities for material by-products from the geothermal brine.

This chapter presents the approach and methods for the LCA and the water quality assessment.

3.1 LIFE CYCLE ANALYSIS

This section describes the assumptions and methodologies used to complete the life cycle inventory for geothermal power production. In assessments of water use at power plants, two water quantities are commonly listed: water withdrawn and water consumed. The former is defined as water taken from ground or surface water sources mostly used for heat exchangers and cooling water makeup, whereas the latter is water either consumed in the combustion process (e.g., in coal and biomass gasification plants — not covered here) or evaporated and hence no longer available for use in the area where it was withdrawn. Water consumption also includes water withdrawals related to construction stage activities (e.g., in drilling muds and cement) in this analysis. The objective is to account for the consumed water — withdrawn water that does not get returned to its area of extraction in liquid form. This analysis does not account for geofluid from the reservoir that is lost but not replaced. Losses to the atmosphere via evaporation at hydrothermal flash plants or to the formation due to reservoir characteristics may impact the long term sustainability of such projects.

3.2 SCENARIOS

Four hypothetical geothermal power plants scenarios were evaluated. Scenarios 1 and 2 consider two sizes of EGS power plants. Scenario 3 involves a comparatively smaller, binary hydrothermal power plant. Scenario 4 is for a larger, flash hydrothermal power plant. Detailed assumptions for the scenarios are listed in Table 3-1.

Table 3-1 compares the scenarios across several design parameters that affect performance, cost, and demands for energy, materials, and water. Each scenario was run in DOE's Geothermal Electricity Technology Evaluation Model (GETEM) repetitively to create a range of possible outcomes according to the parameters in Table 3-1.

TABLE 3-1 Parameter Values for Four Geothermal Power Plant Scenarios

| Parameters | Scenario 1 | Scenario 2 | Scenario 3 | Scenario 4 |
|-------------------------------------|--------------------------|--------------------------|-----------------------------|-------------------|
| Geothermal technology | EGS | EGS | Hydrothermal | Hydrothermal |
| Net power output, MW | 20 | 50 | 10 | 50 |
| Producer to injector ratio | 2 | 2 | 3 or 2 | 3 or 2 |
| Number of turbines | single | multiple | single | multiple |
| Generator type | binary | binary | binary | flash |
| Cooling | air | air | air | evaporative |
| Temperature, °C | 150–225 | 150–225 | 150–185 | 175–300 |
| Thermal drawdown, % y ⁻¹ | 0.3 | 0.3 | 0.4–0.5 | 0.4–0.5 |
| Well replacement | 1 | 1 | 1 | 1 |
| Exploration well | 1 | 1 or 2 | 1 | 1 |
| Well depth, km | 4–6 | 4–6 | <2 | 1.5 <3 |
| Pumping | injection & production | injection & production | injection & production | injection only |
| Pumps, Injection | surface | surface | surface | surface |
| Pumps, Production | submersible 10,000 ft | submersible 10,000 ft | lineshaft or submersible | none |
| Distance between Wells, m | 600–1,000 | 600–1,000 | 800–1,600 | 800–1,600 |
| Location of Plant to Wells | central | central | central | central |
| Geographic Location | Southwest U.S. | Southwest U.S. | Southwest U.S. | Southwest U.S. |
| Plant Lifetime, years | 30 | 30 | 30 | 30 |

3.3 WELL FIELD DEVELOPMENT

The well field includes production wells, injection wells, and the pipelines connecting the production wells to the plant and the plant to the injection wells. A simplified schematic is shown in Figure 3-1. To model the well field, it was assumed that the production wells and injection wells would have the same configurations and depths.

For Scenarios 1 and 2, well designs were based on the 5,000-m EGS wells described in *The Future of Geothermal Energy* (MIT, 2006). For the binary and flash hydrothermal systems of Scenarios 3 and 4, the design configuration of well RRGE2 in Raft River, Idaho, was used (Narasimhan and Witherspoon, 1977). All designs were modified to assess material requirements for wells at various depths, as summarized in a companion report (Sullivan et al., 2010). The well designs were used to determine the amount of materials, water, and fuel required in the drilling, casing, and cementing of a well. The assumptions and methods used for well field development as they pertain to water use are described in the following sections. For details of the methods used to assess material and energy requirements for well construction, refer to the companion report (Sullivan et al., 2010).

3.3.1 Well Construction

The drilling phase of the geothermal power plant life cycle requires the use of drill rigs, fuel, and materials including the casing, cement, liners, mud constituents, and water. Water is used during the well construction stage as drilling fluids and for cementing the casing in place. The assumptions and methods used for construction as they pertain to water use are described in the following sections.

3.3.1.1 Drilling Fluids

During the drilling process, fluids or “muds” are used to lubricate and cool the drill bit, to maintain downhole hydrostatic pressure, and to convey drill cuttings from the bottom of the hole to the surface. To accomplish these tasks, drilling muds contain chemicals and constituents to control factors such as density and viscosity and to reduce fluid loss to the formation. Operators formulate muds on site and alter the recipe according to the physical conditions and chemical properties of the site and as conditions change during drilling. Muds are screened to remove cuttings brought to the surface, and are periodically changed during drilling in response to changing conditions. The mud remaining in the circulation system after drilling may be disposed or regenerated for future use.

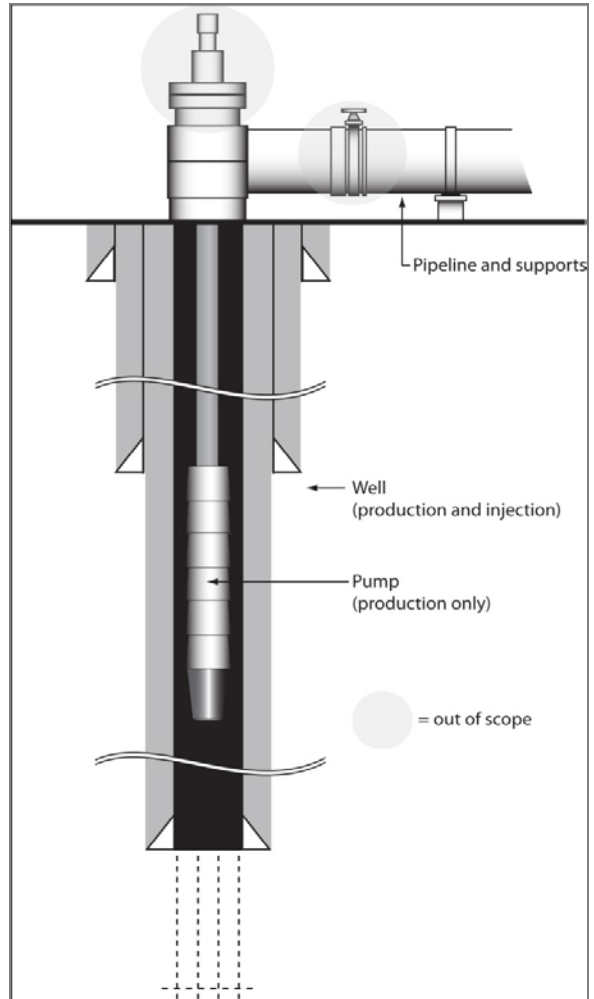


FIGURE 3-1 System Boundary for Well Field

The total volume of drilling muds depends on the volume of the borehole and the physical and chemical properties of the formation. As a result, mud volumes vary, and predicting the volume for a typical drilling project can be challenging. For the purposes of this study, average mud volume data were obtained from the literature (USEPA, 1993; Mansure, 2010). Mud volumes from three wells at various depths between 10,000 and 20,000 ft (3 to 6 km) were obtained, and the ratio of barrels (bbl) of drilling mud to bbl of annular void was found to be 5:1. This assumption was used for the various well depths in the four geothermal scenarios.

For the purposes of the LCA, the drilling fluids were assumed to be water-based muds. Water-based muds are commonly used, and while oil-based muds are used in high-temperature drilling for thermal stability, they require additional handling and treatment after use (USEPA, 1993). A ratio of 1 bbl of water to 1 bbl of drilling mud was assumed. The composition of the mud was provided by ChemTech Services as summarized by Mansure (2010) to provide the required drilling fluid properties. Materials included bentonite, soda ash, Gelex (polyacrylate/polyacrylamide blend), Polypac (polyanionic cellulose polymer), xanthan gum, polymeric dispersant, high-temperature stabilizer, and modified lignite or resin. Because the dominant material by several orders of magnitude was bentonite, the other materials were ignored for this study.

3.3.1.2 Well Casing and Cementing of Casing

The volume of cement needed for each well was determined by the total volume of the well and the volume of the casing and interior. In the well design work of Tester et al. (2006), the larger-diameter casings are specified according to grade and thickness rather than grade and weight per foot, which is the customary method of the American Petroleum Institute (API) (Mansure, 2010). Specification accounts for adequate burst, collapse, and yield strength. For any given grade, the thickness specifies the casing design. The weight per foot and inner diameter can be determined from the thickness and grade. The designs used for this study are summarized in the companion report by Sullivan et al. (2010).

It was assumed that Portland Class G cement (according to API Specification 10A) and Portland Class G cement with 40% silica flour would be used. For Class G cement, the ratio of water volume to slurry volume is 0.58 (5 gal of water are required per 1.15 ft³ or 32.6 L of slurry) (Halliburton, 2006). For Class G cement with 40% silica flour, the ratio of water volume to slurry volume is 0.56 (6.8 gal of water are required per 1.62 ft³ or 45.9 L of slurry) (Halliburton, 2006). Both Class G cement and Class G cement with 40% silica flour are considered for each well design and depth in this LCA.

3.3.2 Hydraulic Stimulation of the Resource

Once a well is in place, water is also used to stimulate the reservoir for EGS projects. Stimulation of the resource was only considered for the EGS well fields, Scenarios 1 and 2. Stimulation opens existing spaces within the formation to enable or enhance the circulation of the geofluid. The stimulation process occurs in a series of steps that all require the pumping of water down the well hole. The first three steps apply to a single well and include prestimulation

test, main stimulation, and post-stimulation test. Typically, stimulation occurs at the point of injection to complete the flow of the geofluid from the injection well to a production well.

More wells are then constructed in the well field to enable complete circulation of the geofluid. Additional stimulation of these wells may be needed but was not considered in this LCA because it is assumed that the production wells would be located within the stimulated flow zone of the injection well. Once these wells are complete, short-term and long-term circulation tests are conducted. Typical water volumes, flow rates, and lengths of time for these steps are shown in Table 3-2. The total required volume of water for all stimulation activities for one well including circulation tests is 42,200–55,400 m³. This assumes that no water is reused.

Published information on EGS stimulation projects and the volumes of fluids used is limited, and available literature values are from international projects with different geological characteristics than potential projects in the U.S. The average volume from literature values was found to be 26,939 m³ (169,440 bbl) of water per well (Asanuma et al., 2004; Michelet and Toksöz, 2006; Zimmermann et al., 2009; Tester et al., 2006). This volume is greater than shale gas hydraulic fracturing efforts in the U.S., which are typically between 7,570 and 15,140 m³ (Ground Water Protection Council & ALL Consulting, 2009).

TABLE 3-2 Water Volume Requirements by Step for Stimulation of One Well

| Step | Flow Rate (kg/s) | Volume (m³) | Length of Time (days) | Source^a |
|------------------------|-----------------------------|-----------------------------------|----------------------------------|---------------------------|
| Prestimulation test | 5–7 | 400–600 | 1 | 1 |
| Main stimulation | 30–70 | 13,000–58,000 | 1–6.4 | 1–5 |
| Post stimulation | 7–50 | 7,200 | 2.5 | 1 |
| Short-term circulation | 20 | 2,600–3,600 | 21 | 1 |
| Long-term circulation | 50–100 | 4,000–13,000 | 21 | 1 |

^a 1 = Tester et al. (2006); 2 = Asanuma et al. (2004); 3 = Entingh (1999); 4 = Michelet and Toksöz (2006); 5 = Zimmermann et al. (2009).

3.4 PIPELINE AND PLANT CONSTRUCTION

A material inventory was also conducted for the construction of the remaining infrastructure. While the material and infrastructure at the wellhead is not included in this assessment (see Figure 3-1 for systems boundary), the pipeline connecting a well to the power plant is included. For this LCA, it was assumed that each production well has a separate pipeline to deliver the geofluid through the plant and to an injection well. Because the producer to injector ratio is greater than 1, an injection well receives multiple pipelines of produced geofluid. The pipelines are aboveground and require support structure. The approach to determining the materials and energy required for construction and installation of the pipeline and power plant are summarized in Sullivan et al. (2010). Water requirements for this infrastructure are summarized below.

3.4.1 Pipeline Supports

On-site water use for pipeline construction is limited to the concrete for the support structures. The number and design of these structures are dependent on the required pipe diameter. The diameter of the pipes was determined first according to the distance between the wells, flow rate of the geofluid, and physical properties of the geofluid. As described in Sullivan et al. (2010), for a pipeline distance of 1,000 m, 8-in. or 10-in.-diameter schedule 40 steel pipe would suffice for all scenarios (20.32-cm and 25.40-cm in diameter). Because the maximum span between supports for 8-in.-diameter schedule 40 steel pipe, 5.8 m (19 ft), is less than the span required for 10-in.-diameter pipe, 6.7 m (22 ft), the span for the 8-in.-diameter pipe was used to determine a maximum estimate of material and water requirements for the pipeline supports (McAllister, 2009).

The material requirements for the foundation include forming tubes, concrete, and rebar. The design for the foundation assumed a hole with a depth of 1.83 m (6 ft) and diameter of 40.64 cm (16 in.) (E-Z Line, 2005). The foundation details are described in Sullivan et al. (2010). As concrete mixes vary considerably, three recipes for controlled low-strength material concrete were selected (IDOT, 2007). All recipes include Portland cement, fine aggregate, and water. Two of the three recipes also include fly ash (Class C or F) (IDOT, 2007). Table 3-3 summarizes the material requirements of the three mixes for one pipeline from a production well to the plant and an injection well.

TABLE 3-3 Material Requirements for Concrete Mix for Foundation Supports for a 1,000-m Pipeline

| Materials | Mix 1 | Mix 2 | Mix 3 |
|---|--------------|--------------|--------------|
| Portland cement (metric ton) | 1.2 | 2.9 | 0.9 |
| Fly ash – Class C or F (metric ton) | 2.9 | 0.0 | 2.9 |
| Fine aggregate – saturated surface dry (metric ton) | 68.2 | 58.8 | 58.8 |
| Water (gal) | 3,371 | 2,593 | 2,593 |

3.4.2 Power Plant Construction

Water volumes for plant construction were limited to on-site use for concrete. A typical concrete recipe requires approximately 200 g/L of water/concrete (Kendall, 2007). To determine the total amount of concrete for the four scenarios, two sets of results were generated using the Icarus Process Evaluator, which enables the estimation of costs, components, and materials for building new production facilities. The material and water estimates for the concrete for each scenario are summarized in Table 3-4.

TABLE 3-4 Material and Water Requirements for Geothermal Power Plant Construction

| Materials | Metric Tons | | | |
|-----------|-------------|-----------|--------------|-------------|
| | EGS 20-MW | EGS 50-MW | Binary 10-MW | Flash 50-MW |
| Cement | 1,924 | 4,809 | 960 | 1,631 |
| Gravel | 3,807 | 9,517 | 1,899 | 3,227 |
| Sand | 2,658 | 6,645 | 1,326 | 2,254 |
| Water | 812 | 2,029 | 405 | 688 |

3.5 OPERATIONS

The vast majority of water used during operations is used to generate electricity. This water, which is extracted from the resource, is commonly referred to as the geofluid. In binary systems, the geofluid is reinjected into the reservoir. In a flash system, geofluid that is flashed to vapor is released to the atmosphere and the condensed geofluid is returned to the reservoir. In addition to electricity generation, water is used to condense vapor for (1) reinjection in the case of the geofluid or (2) reuse in the case of the working fluid in binary systems. Water is also used in normal operations to manage dissolved solids and minimize scaling.

The total flow rate of geofluid through the plant depends on the flow rate produced from each well and the total number of production wells. According to historical data from the California Division of Oil, Gas, and Geothermal Resources, typical production rates vary according to the temperature of the resource, but for binary plants are 393,000–512,000 gal/day per megawatts of electricity produced (MWe), and for secondary flash plants, those that flash the condensate a second time prior to reinjection, are 93,000–171,000 gal/day/MWe. Production volumes for the scenarios in this study were determined by using GETEM. Average production volumes for this study, according to the temperature ranges presented in Table 3-1, are shown in Table 3-5.

TABLE 3-5 Average Flow Rates for Four Geothermal Scenarios

| Scenarios | Daily Flow Rate | |
|--------------|-----------------|-------------|
| | gal/day | gal/day/MWe |
| 20-MW EGS | 8,688,000 | 434,000 |
| 50-MW EGS | 21,671,000 | 433,000 |
| 10-MW binary | 6,096,000 | 610,000 |
| 50-MW flash | 23,301,000 | 466,000 |

3.5.1 Makeup Water

To determine potential makeup water requirements, monthly historical production and injection volumes for geothermal power plants were analyzed (CDOGGR, 2010). Available production and injection data were analyzed to determine typical makeup and loss rates, as shown in Table 3-6.

TABLE 3-6 Average Flow Rates from Historical Production and Injection Data for Several California Geothermal Power Plants (CDOGGR, 2010)

| Site | Category ^a | Average flow rates (gal/day) | | | |
|-------------|-----------------------|------------------------------|------------|-----------|------------|
| | | Production | Injection | Makeup | Loss |
| Casa Diablo | Binary | 14,317,000 | 13,980,000 | (219,000) | 556,000 |
| East Mesa | Binary | 46,091,000 | 44,198,000 | (204,000) | 2,248,000 |
| Heber | Binary | 35,386,000 | 33,126,000 | (22,000) | 2,282,000 |
| Coso | Multi-stage flash | 25,195,000 | 13,113,000 | (6,000) | 12,088,000 |
| Salton Sea | Multi-stage flash | 53,381,000 | 43,664,000 | (15,000) | 9,648,000 |

^a Some plants may generate electricity from both binary and flash systems. The *category* designation represents the majority type of generators at a particular site.

While the losses for the three binary systems in Table 3-6 range from 3.9% to 6.4% of the production rate, the binary sites with larger loss rates (East Mesa and Heber) also include sites with flash turbine systems and rely on wet-cooling (DiPippo, 2008). Casa Diablo is air-cooled (Campbell, 2000); however, beginning in 2000, two evaporative cooling systems were used in conjunction with air cooling to maximize energy performance during summer months (Smith, 2002). As average injection and production flow rates differed at Casa Diablo prior to 2000, there are unaccounted operational consumptive water losses in addition to the evaporative cooling described by Smith (2002). For sites with flash and multi-stage flash systems, geofluid loss rate is typically larger than binary systems, because the geofluid is directly flashed in addition to evaporative cooling losses. For the purposes of this study, the multi-stage flash system loss and makeup rates (e.g. Coso and Salton Sea) were assumed to be applicable to the flash scenario.

3.5.2 Cooling Water

In conventional thermoelectric power generation, water is primarily used in cooling to condense steam. In *Energy Demands on Water Resources: Report to Congress on the Interdependency of Energy and Water*, thermoelectric cooling water needs for geothermal power plants were reported at 2,000 gal/MWh for withdrawal and 1,400 gal/MWh for consumption (DOE, 2006). These estimates were based on The Geysers power plant, the only one in the U.S. to use a dry steam field. While this assumption is valid and appropriate because The Geysers is the largest and supplies nearly 58% of the electricity generated by geothermal power in the U.S.,

the majority of electricity-generating geothermal units within the U.S. are binary. Figures 3-2 and 3-3 show the breakdown of U.S. geothermal production by unit type.

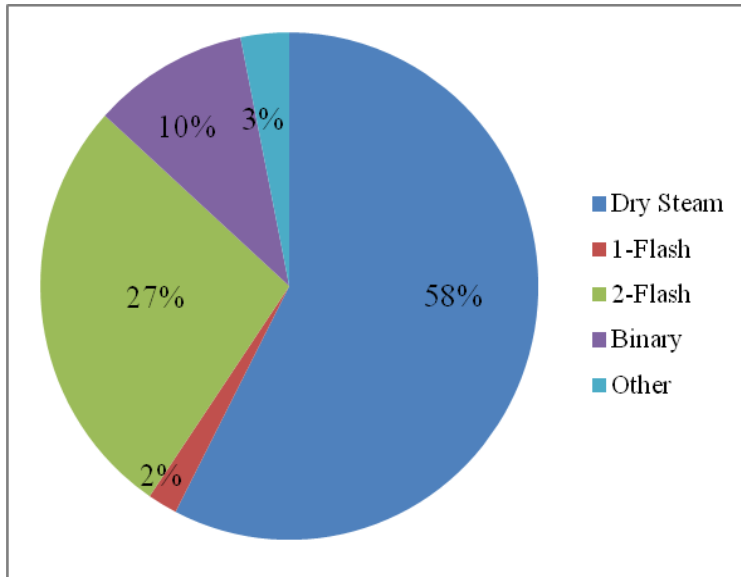


FIGURE 3-2 Percent of U.S. Geothermal Power Production Capacity in 2007 by Technology (DiPippo, 2008)

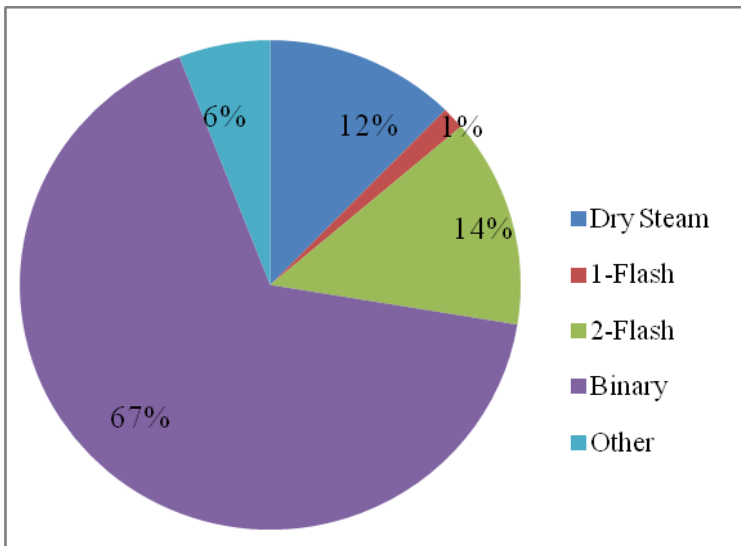


FIGURE 3-3 Percent of Total U.S. Geothermal Power-Generating Units by Technology

Cooling water withdrawal and consumption estimates are not the same for flash and binary power plants because of differences in vapor temperature, total mass of vapor requiring condensing, and the condensation point for working fluids in binary plants. Adee and Moore (2010) reported a volume of less than one-fifth the estimated water withdrawn for flash systems in the Salton Sea. The volume consumed is about one-fourth for The Geysers according to DOE (2006). Adee and Moore (2010) reported use volumes for a water-cooled binary plant assuming once-through cooling and found water withdrawn was nearly a factor of 2 greater than for The Geysers and water consumed was a factor of 3 greater. Because the geothermal industry is moving toward air-cooled binary systems, water-based cooling was not considered for the binary hydrothermal scenario or the EGS scenarios.

3.6 WATER QUALITY

To assess the water quality of typical geofluids, a search was performed to obtain chemical composition data. A total of five datasets were obtained (see Table 3-7).

The five datasets were merged into a single database to facilitate further analysis. The original datasets were taken as-is with minimal quality control. This is not always a good assumption, especially given the age of some of the data, much of which were collected in 1950–1980; however, it is the best data available and further quality control would have been beyond the scope of this effort. Only the NatCarb brine data were trimmed because the original dataset contained over 125,000 samples, many of which were not near geothermal sources. Only samples with temperatures above 90°C from this dataset were included in the merged database. The complete merged database is referred to as the Argonne Geothermal Geochemical Database (AGGD) to differentiate it from its component datasets. Details of the format and contents of the AGGD are given in Appendix A. The complete database can be downloaded at www.anl.gov/renewables/research/geothermal.html.

The AGGD was organized different ways to facilitate different analyses. In general, data were organized by temperature on the basis of USGS designations of low-temperature (<90°C), moderate-temperature (90°C–150°C), and high-temperature (>150°C) geothermal sources (Duffield and Sass, 2003). Because many records did not include a temperature value, approximately 2,300 moderate-temperature data points and 800 high-temperature data points were used for most of the analyses. Appendix C contains chemical analyses for the complete data set.

The results of the water quality analysis are detailed in Chapter 5. The analysis includes geofluid composition, gas composition, analysis of scale and corrosion potential, human health risks and comparison with drinking water standards, and potential for mineral extraction and other beneficial uses.

TABLE 3-7 Geofluid Chemical Composition Data Sources

| Name | Organization | Description | Size |
|--|--|---|--------------------|
| Mariner Database (chemical and isotope data) ^a | USGS | Contains chemical data collected over a period of 40 years by USGS researchers. Samples were taken from hot springs, mineral springs, cold springs, geothermal wells, fumaroles, and gas seeps. | 3,252 |
| Great Basin Groundwater Geochemical Database (GBGGD) ^b | Great Basin Center for Geothermal Energy | Contains geochemical data from groundwater samples in the Great Basin, Nevada. It includes both hot and cold water samples. | 47,512 |
| Nevada Low-Temperature Geothermal Resource Assessment ^c | Nevada Bureau of Mines and Geology | An inventory of low- and moderate-temperature geothermal resources in Nevada. Contains some basic geochemical data. | 455 |
| NatCarb (brine data) ^d | Kansas Geological Survey | Large database of brine chemistry compiled for the DOE National Energy Technology Laboratory NatCarb carbon sequestration database. | 1,170 ^f |
| GEO THERM ^e | USGS/Nevada Bureau of Mines and Geology | A geothermal geological and geochemical database developed in the 1970s and maintained until 1983. | 1,125 |

^a Mariner (2010) and USGS (2006).

^b CGBCGE (2010).

^c Garside (1994).

^d Moore (2010).

^e USGS (1983).

^f Full database contains 125,000+ samples; only those with temperature greater than 90°C were used for this study.

4 RESULTS OF THE LIFE CYCLE ANALYSIS

To estimate the volume of water needed for each scenario, the total numbers of wells for each scenario were determined through GETEM simulations. Multiple simulations were run varying the input parameters according to the ranges provided in Table 3-1 to determine the average number of production and injection wells for each scenario. The results are provided in Table 4-1.

TABLE 4-1 Average Number of Wells by Scenario

| Scenarios | Production Wells | Injection Wells | Total Wells |
|--------------|------------------|-----------------|-------------|
| 20-MW EGS | 6.3 | 3.2 | 9.5 |
| 50-MW EGS | 15.8 | 7.9 | 23.7 |
| 10-MW binary | 3.0 | 1.2 | 4.2 |
| 50-MW flash | 14.6 | 6.0 | 20.6 |

For the sizes of the EGS power plants considered in this scenario, the number of wells scales linearly. Whereas the temperatures for the binary plant were similar to those evaluated for EGS, the higher average flow rate considered for the binary hydrothermal scenario resulted in fewer wells needed per megawatt electricity produced. The higher temperatures for the flash hydrothermal scenario similarly resulted in fewer wells needed than for the 50-MW EGS scenario. With this information from GETEM, water volume requirements could be determined for each life cycle stage for each scenario. What follows is a summary and discussion of the LCA of water use. The scenario results are tabulated by life cycle stage in Appendix B.

4.1 CONSTRUCTION AND STIMULATION

The water required for each life cycle stage was aggregated for each scenario. Figure 4-1 presents the construction stage water requirements for the four geothermal scenarios.

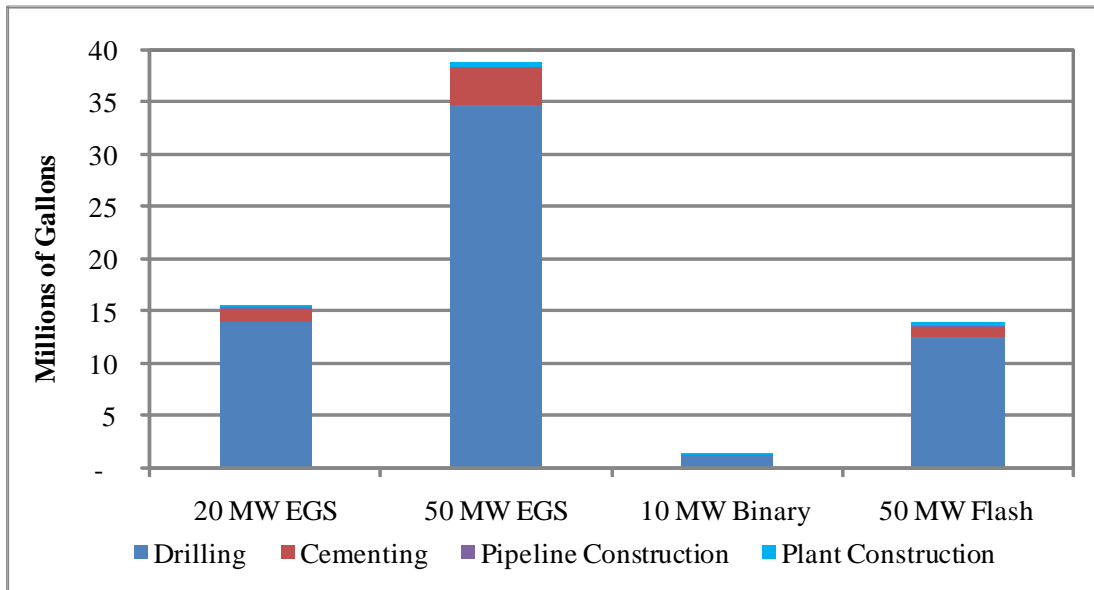


FIGURE 4-1 Volume of Water Consumed for Construction of Geothermal Power Plants according to Scenarios and Assuming Average Depth for Wells

The construction stage accounts for drilling wells, cementing casing into place, and laying the concrete foundations for the pipeline supports and the power plant. Figure 4-1 shows that the largest volume of water for all four scenarios is used for drilling wells, and the second largest volume is attributable to cementing the well casing into place. Because the EGS wells are much deeper on average than the hydrothermal scenario wells, the water requirements per well are much higher. Well depths that are more than twice those of the hydrothermal wells explain the similar water requirements for the 20-MW EGS and the 50-MW flash plant, even though there are many more wells required for the flash plant. The water volumes required for the concrete in the power plant construction and the pipeline support foundations are significantly less than the volumes required for well construction.

Figure 4-1 presents drilling volume estimates for the average depth within the depth range of each scenario (see Table 3-1). The difference in water requirements due to depth for the two EGS scenarios is shown in Figure 4-2. It is apparent that both depth and the total number of wells affect water volume requirements in drilling and cementing.

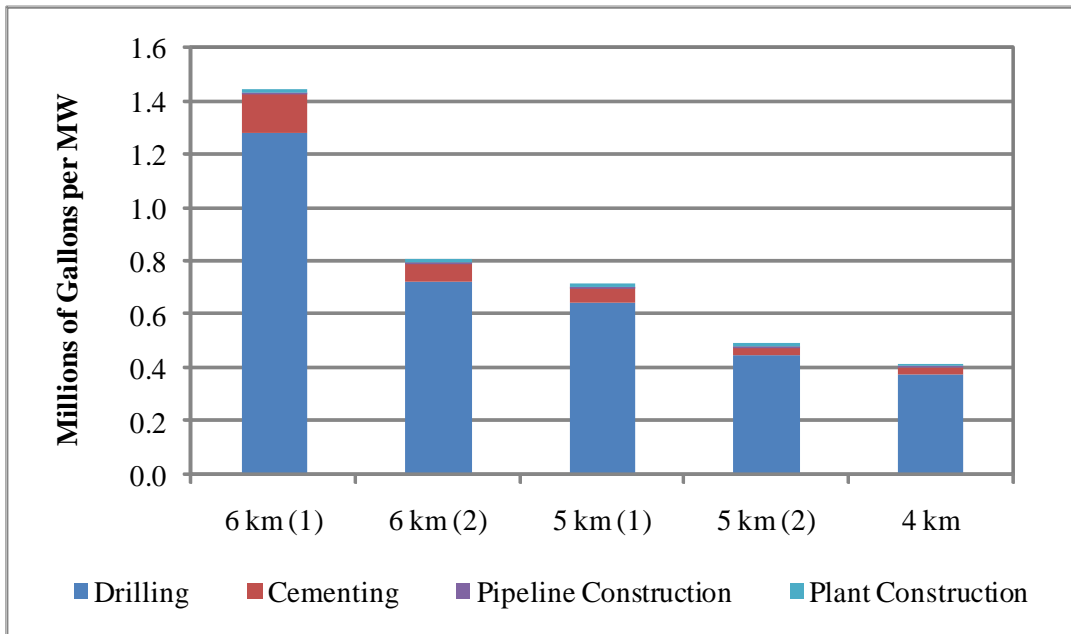


FIGURE 4-2 Water Consumption in Millions of Gallons per Megawatt as a Function of Well Depth for the Construction Stage of the EGS Scenarios

For the EGS scenarios, water is required for stimulating the reservoir in addition to being required during the construction stage. No stimulation was assumed for the two hydrothermal scenarios. According to Figures 4-3 and 4-4, the stimulation stage requires the majority of the water for the EGS scenarios, regardless of depth. Stimulation volume is assumed to be dependent on the desired water volume flow rate (a function of plant capacity) and to be independent of depth. The water volume required for stimulation contributes approximately 60%–80% of total upfront water requirements for the evaluated well depths. Water requirements for stimulation can vary from those presented here according to: (1) number of stimulations required for successful circulation and (2) reuse of water for multiple stimulations.

4.2 PLANT OPERATIONS AND THE LIFE CYCLE

Assuming a plant lifetime of 30 years, the total volume of water for each scenario for all stages of the life cycle is shown in Figure 4-5. For this study, we focused on air-cooled systems for the hydrothermal binary scenario and the two EGS scenarios. Wet-cooling was assumed for the flash system, with steam condensate provided by the geofluid used for cooling. As shown in Table 3-6, nearly half of the geofluid loss in the air-cooled binary system is replaced with makeup water. For the EGS scenarios, it was assumed that at least the same volume would need to be replaced with makeup water, with the potential need to replace all lost geofluid to maintain reservoir pressure. Therefore, Figure 4-5 presents a range of operational water volumes for the EGS scenarios. Makeup water during the operations phase is the predominant water use for all scenarios.

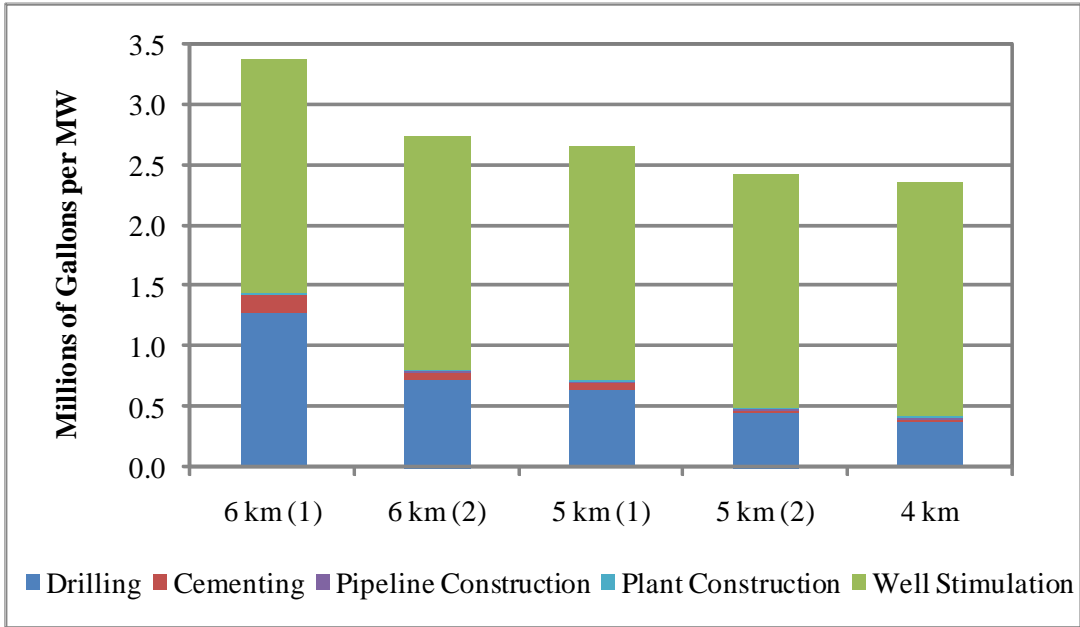


FIGURE 4-3 Water Volume in Millions of Gallons per Megawatt Consumed for the EGS Scenarios According to Depth

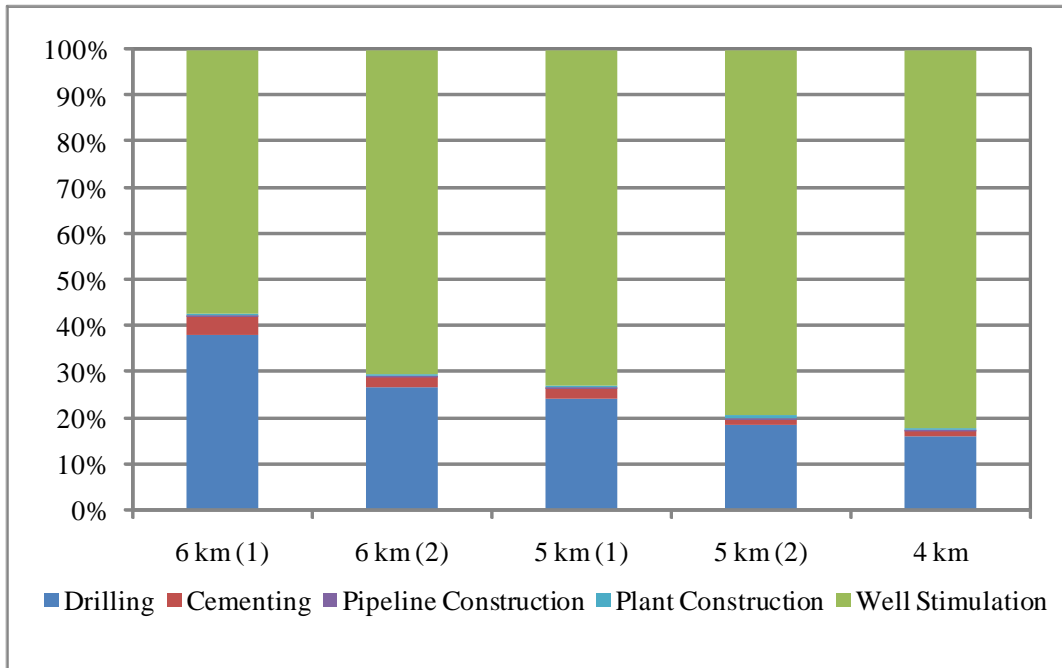


FIGURE 4-4 Contribution to Total Water Consumption by Process

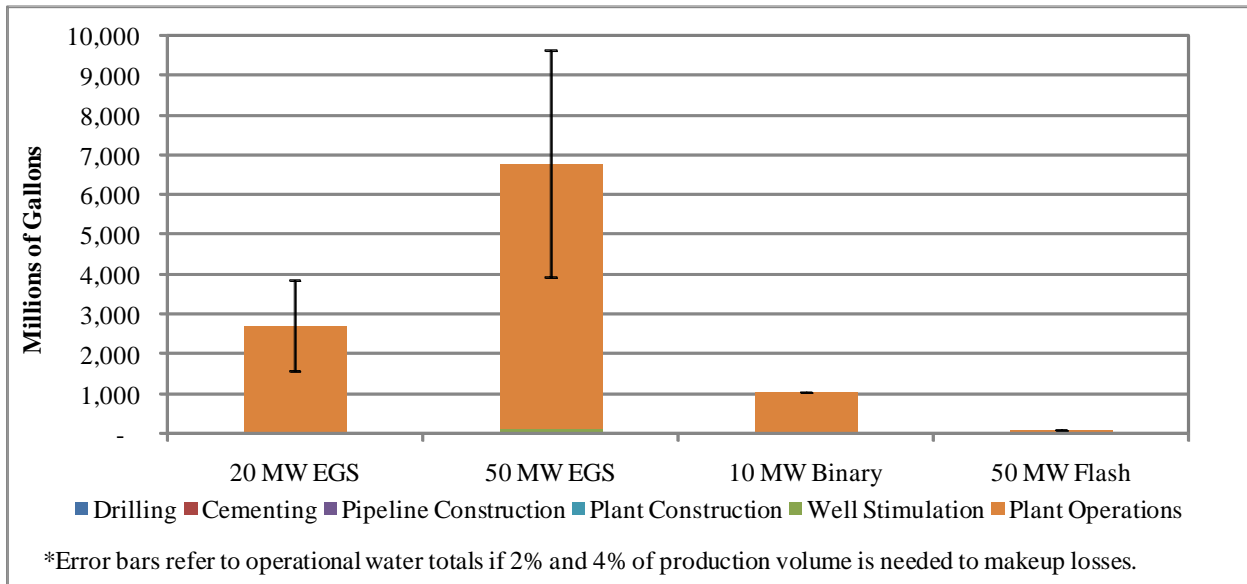


FIGURE 4-5 Life Cycle Volume of Water Consumption in Millions of Gallons for Geothermal Power Plant Scenarios

The contribution of the operations stage water for each scenario is shown in Figure 4-6. It is apparent that the vast majority of water use occurs during the operations phase. Only the flash power plant has another water use requirement greater than 2%. The drilling fluid requirements for the flash plant are responsible for 14% of the life cycle water volume required.

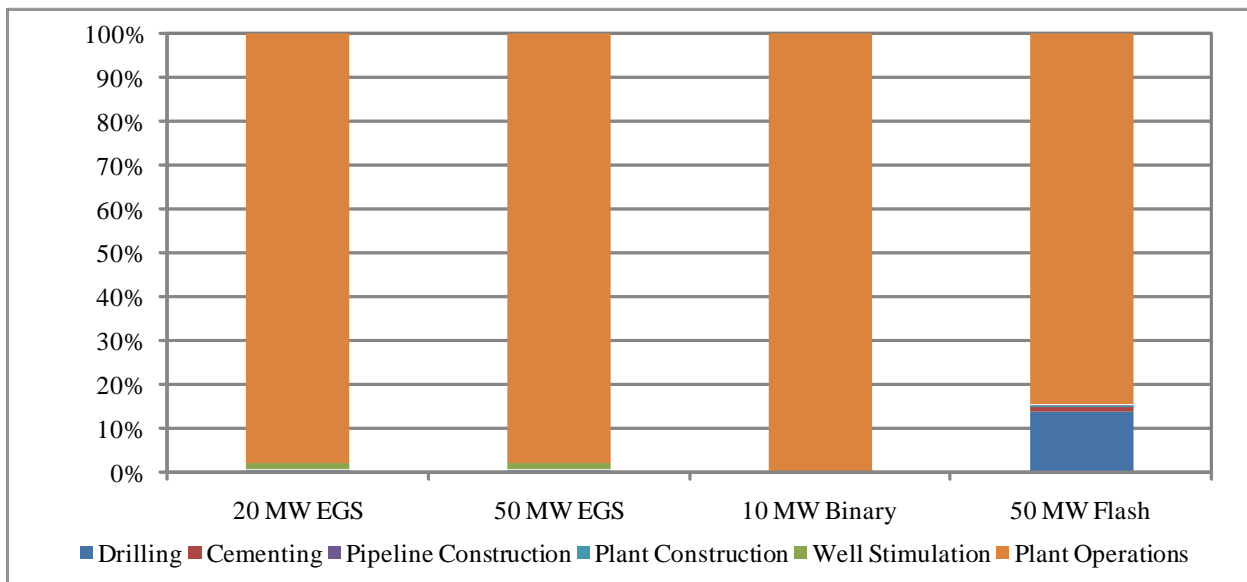


FIGURE 4-6 Contribution of Operations Water Use to Total Water Use in the Power Plant Life Cycle

Normalizing the scenarios per kilowatt-hour of lifetime energy output, Table 4-2 shows that the two EGS scenarios have similar water use per kilowatt-hour while the hydrothermal scenarios use much less water per kilowatt-hour than the EGS scenarios in both life cycle stages.

TABLE 4-2 Average Water Consumption Estimates for Geothermal Power Generation by Life Cycle Stage over Plant Lifetime in Gallons per Kilowatt-Hour of Lifetime Energy Output

| Scenario | Construction and EGS Stimulation (gal/kWh) | Operations (gal/kWh) | Total (gal/kWh) |
|-----------------|---|-----------------------------|------------------------|
| 20-MW EGS | 0.01 | 0.29–0.72 | 0.30–0.73 |
| 50-MW EGS | 0.01 | 0.29–0.72 | 0.30–0.73 |
| 10-MW binary | 0.001 | 0.27 | 0.27 |
| 50-MW flash | 0.001 | 0.01 | 0.01 |

Adee and Moore (2010) reported that freshwater used for cooling at the Salton Sea hydrothermal flash power plants is 0.36 gal/kWh. However, this is an exception. Water cooling towers are typically used for flash plants, because these plants provide much of the needed water from steam condensate (DiPippo, 2008). The power plant modeled in GETEM assumes that the cooling tower relies on the steam condensate generated after the geofluid is flashed. According to GETEM, the single-stage flash power plant modeled would lose an average 2.7 gal/kWh from the reservoir due to evaporation, drift, and blowdown. Reliance on the geofluid for cooling reduces the makeup water requirements for operations. However, the geofluid loss over the lifetime may decrease the sustainability of the reservoir.

Adee and Moore (2010) also reported on operational water use for a binary system in the Salton Sea geothermal area that operates using once-through cooling and withdraws 4.45 gal/kWh. Frick et al. (2010) conducted an LCA on enhanced low-temperature binary systems that rely on wet-cooling and found operational water consumption to be 0.08 gal/kWh assuming an average conversion efficiency of 10.5%. The operational water use for the binary and EGS systems are not attributable to cooling because the power plants are air cooled. This typical operational makeup water volume is based on an operating air-cooled binary plant. Typical operations and maintenance activities including maintenance of reservoir pressure or switching to evaporative cooling during summer daytime operations may be responsible for makeup volume requirements.

For the overall life cycle, the consumption for EGS power plants for this study is similar to Frick et al. (2010), who provided component estimates of consumption that aggregate to 0.36 gal/kWh over the lifetime energy output. However, Frick et al. (2010) identifies the construction stage, particularly well stimulation referred to as “reservoir enhancement,” as the stage primarily responsible for the water consumption requirements. If reservoir enhancement includes makeup water to address declining geofluid water volumes over time, some of the

volume may be accounted for in the makeup water requirements identified in the operations stage of the EGS power plant life cycles presented here.

Makeup water requirements due to reservoir losses were not specifically included for the EGS scenarios. While subsurface water loss is a parameter that can be input directly to GETEM to model its effect on plant performance and makeup water requirements, there is currently insufficient empirical data to ensure the accuracy of estimating the effects of reservoir losses in this way.

Makeup water during operations would not need to be freshwater. Makeup water could come from saline sources such as nearby saline aquifers, water from oil and gas production, saline water extracted from carbon capture and storage reservoirs, and treated municipal wastewater.

4.3 COMPARISON WITH OTHER POWER PLANT TYPES

Most electric power plants require water to some degree for operation. In the U.S. around 40% of all freshwater withdrawals are for thermoelectric application (GAO, 2009). For conventional power plants, water is used in the steam turbine, for removing waste heat from the plant, and, in gasification facilities, as a source of hydrogen in syngas production for combustion in gas turbines. Hydroelectric facilities are totally dependent on water, though it can be supplied by either a reservoir or run-of-the-river. For geothermal plants, water is used for well field and power plant construction, and in some cases it is used for cooling. For all geothermal plants, geothermal fluid is produced from the ground. This is often saline water and in some cases steam.

Table 4-3 presents an overview of water use for various electricity generation technologies. More detailed water use information can be found in Appendix B. Reported literature values typically focus on the operational stage of electrical power plant life cycles. However, there are two exceptions where water consumption in other life cycle stages is considered significant. The first is the construction stage of geothermal plants. Because a considerable amount of water is consumed for drilling wells during plant construction, those amounts are included in our water accounting. The second is the production stage of the fuels used to power electricity-generating plants. Irrigation water is typically used to grow the necessary energy crops to fuel a biomass electricity-generating plant. Also, a significant amount of water is required to mine and process coal, natural gas, and nuclear fuels.

TABLE 4-3 Aggregated Water Consumption for Electric Power Generation at Indicated Life Cycle Stages in Gallons Per kWh of Lifetime Energy Output^a

| Power Plant | Fuel Production | Plant Construction | Plant Operations | Total Life Cycle^b |
|--------------------------------|------------------------|---------------------------|-------------------------|-------------------------------------|
| Coal | 0.26 | - | 0.004–1.2 | 0.26–1.46 |
| Coal with carbon capture | 0.01–0.17 | 0.13–0.25 | 0.5–1.2 | 0.57–1.53 |
| Nuclear | 0.14 | - | 0.14–0.85 | 0.28–0.99 |
| Natural gas conventional | 0.29 | - | 0.09–0.69 | 0.38–0.98 |
| Natural gas combined cycle | 0.22 | - | 0.02–0.5 | 0.24–0.72 |
| Hydroelectric (dam) | - | - | 4.5 | 4.5 |
| Concentrated solar power | - | 0.02–0.08 | 0.77–0.92 | 0.87–1.12 |
| Solar photovoltaic | - | 0.06–0.15 | 0.006–0.02 | 0.07–0.19 |
| Wind (onshore) ^c | - | 0.02 | 3.62E-08 | 0.01 |
| Geothermal EGS | - | 0.01 | 0.29–0.72 | 0.3–0.73 |
| Geothermal binary ^d | - | 0.001 | 0.08–0.27 | 0.08–0.271 |
| Geothermal flash ^d | - | 0.001 | 0.005–0.01 | 0.01 |
| Biomass | - | - | 0.3–0.61 | 0.3–0.61 |

^a Sources: Adey and Moore (2010), Maulbetsch and DiFilippo (2006), Frick et al. (2010), Gleick (1994), Goldstein and Smith (2002), Harto et al. (2010), NETL (2005), NETL (2008), Vestas Wind Systems A/S (2006).

^b Reported when provided, otherwise summed from values in table.

^c Assumes recovery of water in the end-of-life management stage.

^d Assumes water consumed as makeup for operational loss is a small percentage of total operational geofluid loss.

The results in Table 4-3 are derived from a core set of references that have been widely cited. For example, a recent U.S. Government Accountability Office study used values published by the Electric Power Research Institute (EPRI) (GAO, 2009; Goldstein & Smith, 2002). While withdrawals from water resources (surface or ground) are largest for the “once-through” cooling systems, consumption is typically greatest for cooling tower and pond cooling systems. Almost all water withdrawal and consumption associated with the operation of thermoelectric facilities is for cooling.

Another source cited in Table 4-3 is a DOE study that was conducted as a theoretical modeling effort focusing primarily on advanced electric generation technology such as integrated gasification combined cycle (IGCC), pulverized coal, and natural gas combined cycle (NGCC) (NETL, 2005). The waste heat from all plants studied is ultimately rejected from the plant through evaporative mechanical draft cooling towers at the end of recirculating water systems. The approach taken in the EPRI study was to establish typical ranges of values for each cooling system type for the different types of power plants (Goldstein & Smith, 2002). Those data were derived from statistics published by regulatory agencies, EPRI reports, industry associations, and engineering handbooks. A recent California study on “water use in power” focused on combined cycle systems cooled either with wet cooling systems or dry cooling systems (Maulbetsch and

DiFilippo, 2006). Like for some of the other studies discussed above, results were based on modeling output; actual data from power plants were apparently not used.

The National Energy Technology Laboratory (NETL) also conducted a study that contains useful water consumption data, *Cost and Performance Baseline for Fossil Energy Plants* (NETL, 2007). The study focused solely on coal and natural gas electricity plants. Like many of the other studies just discussed, its results were also derived from a model, in this case, the AspenPlus model. The runs provided material and energy balances from which design detail was derived, along with equipment lists. Operating performance and process limits were based on information in published reports, vendor and user correspondences, design and build performance data, and/or best engineering judgment. NETL has also conducted a more general study on water use in thermoelectric plants (NETL, 2008). In this study they employed NETL Coal Plant Database information along with data from EIA forms 767 and 860. These forms must be filled out annually by any power plant of 10 MW capacity or greater, providing detailed information on plant operation including fuel consumption, ash removal, water withdrawal and consumption. Their “models” are actually data-driven representations of a limited set of power plant types with associated cooling technologies.

A study by Harto et al. (2010) considered life cycle water use of low-carbon transport fuels, which included electric power generation for electric vehicles. Three technologies were considered: solar photovoltaics (PV), concentrated solar power (CSP), and coal with carbon capture. The hybrid LCA relied on both economic input-output models and process-based information to provide low and high estimates for water use. In addition to the life cycle categories in Table 4-9, Harto et al. (2010) accounted for water use attributable to transmission losses, which are included in the numbers reported under total life cycle in Table 4-3.

Water use in wind energy generation has largely been ignored in LCA because water is not consumed when electricity is generated via wind turbines. A study by Vestas Wind Systems A/S (2006) accounted for water, but it is unclear whether the volume reported is throughput or consumption. Assuming that the reported value, 0.01 gal/kWh, is for water consumed, the majority would be during production of the turbines (Vestas Wind Systems A/S 2006).

The total life cycle water consumption reported in Table 4-3, except for the water consumption rate of hydrothermal electric power generation, is visually presented in Figure 4-10. Gleick (1992) estimated the water consumption rate of hydrothermal electric power generation at several times higher than other conventional technologies due to evaporative losses. With the exception of coal with carbon capture, all electric-generating technologies in Figure 4-7 are reported in the literature to consume less than 1 gallon of water per kilowatt hour of lifetime energy output on average. Average values of consumption for coal, nuclear, and conventional natural gas power plant systems are higher than for geothermal scenarios. However, because consumption depends on cooling technology, it is not surprising that reported low consumption values for thermoelectric technologies including coal, nuclear, conventional natural gas, NGCC, EGS, and biomass are similarly near 0.3 gal/kWh. With the exception of geothermal flash, which primarily relies on the geofluid in the reservoir for cooling, PV appears to be more water efficient, with consumption estimates of 0.07–0.19 gal/kWh. Overall, the geothermal

technologies considered in this study appear to consume less water on average over the lifetime energy output than other power generation technologies.

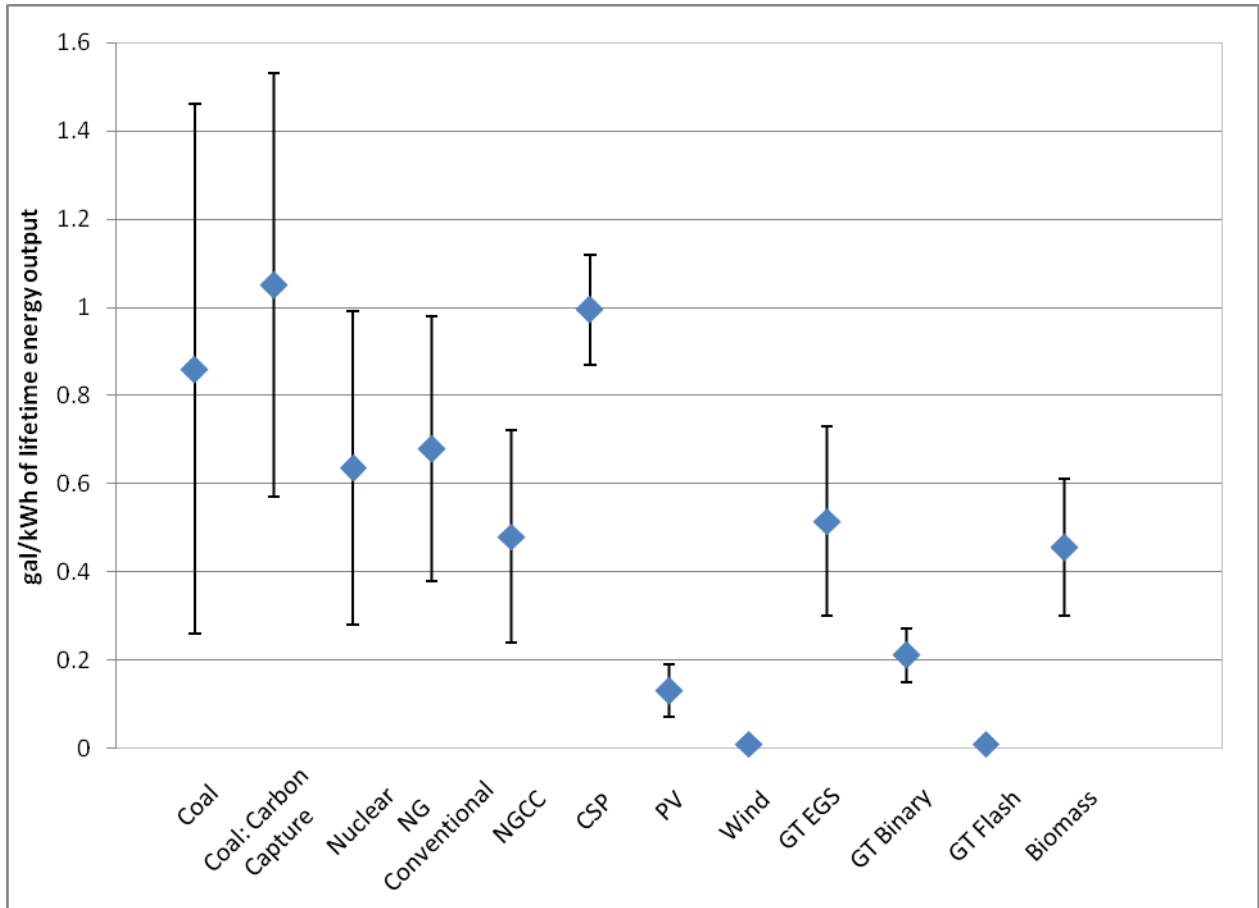


FIGURE 4-7 Water Consumption for Electric Power Generation (Hydropower is not included because it is difficult to allocate evaporative losses from reservoir surfaces to electricity generation. GT Binary and GT Flash estimates assume water consumed as makeup for operational loss is a small percentage of total operational geofluid loss.)

5 ANALYSIS AND INTERPRETATION OF WATER QUALITY

The chemical composition of geofluids varies widely between geothermal fields, within geothermal fields, and even, in some cases, over time within the same geothermal well. The exact chemical makeup of the geofluid can have important implications for both the design and operation of a geothermal plant and its potential environmental impact. The geofluid geochemical data aggregated in the AGGD described in Chapter 3 was used to explore these implications.

The AGGD data were analyzed for a number of key characteristics:

- General chemical composition of geofluids,
- Potential risks of geofluids to water and soil quality,
- Role of dissolved noncondensable gases in both operational considerations and in risk of air pollution,
- Operational concerns based on geofluid composition, including scale and corrosion, and
- Potential for geofluids to be “mined” for valuable minerals.

5.1 GEOTHERMAL BRINE CHARACTERISTICS

The data in the AGGD were statistically analyzed to better understand the range of conditions that may be encountered when dealing with geothermal fluids. In addition to temperature, the pH, total dissolved solids (TDS), and concentrations of various chemical constituents are important to consider when designing or operating a geothermal system.

Figures 5-1 and 5-2 show the distribution of pH and TDS in the AGGD. These two histograms represent all samples in the dataset with temperatures greater than 90°C. The data have not been weighted to account for the fact that many samples are from the same geothermal fields and in some cases from the same geothermal well. When interpreting the graphs, the number on the x-axis represents the upper limit of the bin. For example, in Figure 5-1 the bin labeled “7” represents all samples with a pH from 6.5 to 7.

The pH values appear to be roughly normally distributed around a median of 7.3, with most values falling between 5 and 10. The range of the data varies from as low as 0.9 to as high as 11.8. TDS values are less neatly distributed, with 80% of samples with a value less than 5,000 mg/L and 10% of samples with a value greater than 200,000 mg/L (all of the latter samples were from wells in California).

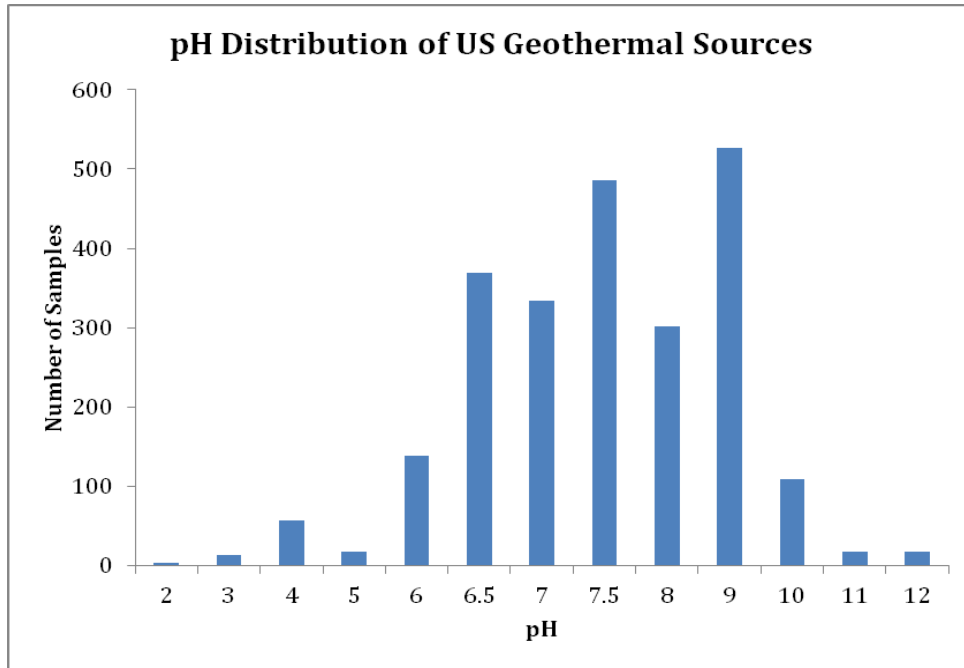


FIGURE 5-1 Distribution of pH Measurements for U.S. Geothermal Sources with Temperatures > 90°C

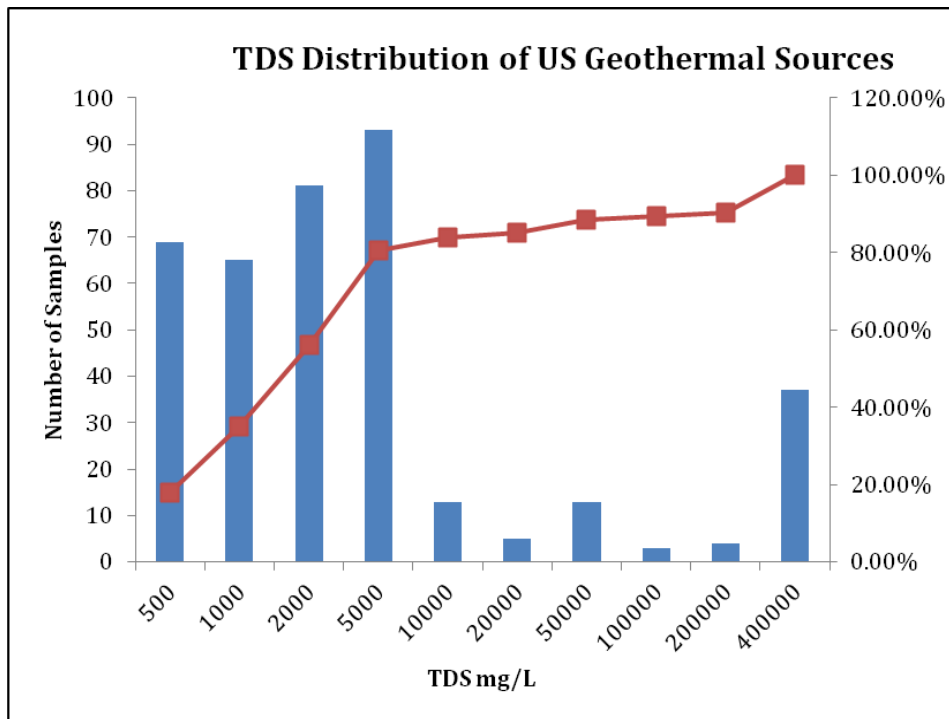


FIGURE 5-2 Distribution of TDS Measurements for U.S. Geothermal Sources with Temperatures > 90°C

Figures 5-3 and 5-4 are box plots representing the distributions of concentrations of chemical constituents found in the data for samples with temperatures greater than 90°C within the AGGD. Figure 5-3 contains the most common constituents while Figure 5-4 contains the less common or lower-concentration constituents. The whiskers of the box plots represent the range of the data.

The dissolved solids in most geofluids are predominantly sodium chloride, followed by bicarbonate, sulfate, silica, calcium, and potassium. The concentration of a constituent can vary by at least an order of magnitude between the 25th and 75th percentile and by as many as five or more orders of magnitude between the extremes of the distribution. Numerical values of the median, mean, and total number of samples are presented for each constituent and for different temperature ranges in Appendix C.

Figure 5-5 shows the chemical compositions of selected AGGD samples. The samples cover a range of geographical locations, temperatures, and pH. In all four cases the constituents listed above constituted at least 95% of the dissolved solids; however the distribution of them varied significantly between samples. Even between Figures 5-5a and 5-5b which represent samples taken from different wells within the same geothermal field in California, the composition varied fairly significantly, with much higher relative concentrations of silica, sulfate, and bicarbonate in the sample from the second well. Additional samples are profiled in Appendix C. They show a similar pattern of the same major constituents but significant variability in the relative concentrations. In general, the concentrations of the anions appear to vary more than the concentrations of the cations.

5.2 WATER POLLUTION POTENTIAL

If not handled responsibly, geofluids are a potential source of water and soil contamination due to elevated TDS and the presence of toxic minerals. Proper well drilling processes and blowout prevention controls are extremely important for minimizing these risks (Tonnessen, 1975). Well casing failure, pipeline leakage, and other surface spills are also possible pathways for contamination, although these can be virtually eliminated through proper design and engineering controls (Tester et al., 2006). To further analyze the potential risk posed by the release of geofluids, the geofluid composition data from the AGGD were compared with U.S. drinking water standards.

U.S. drinking water standards are broken down into primary and secondary standards. The primary standards relate to human health effects and are hard requirements. The secondary standards relate to cosmetic and aesthetic properties such as color, odor, and taste and are strong recommendations but not requirements. Tables 5-1 and 5-2 compare geofluid contaminant concentrations with the primary and secondary EPA drinking water standards, respectively, for inorganic chemicals (USEPA, 2010). The comparison in both tables is broken down into high-temperature (>150°C) and moderate-temperature (90°C–150°C) geofluids. Mean and median concentrations are presented for each contaminant, along with the fraction of the total number of samples in the AGGD that meets the specified drinking water standard.

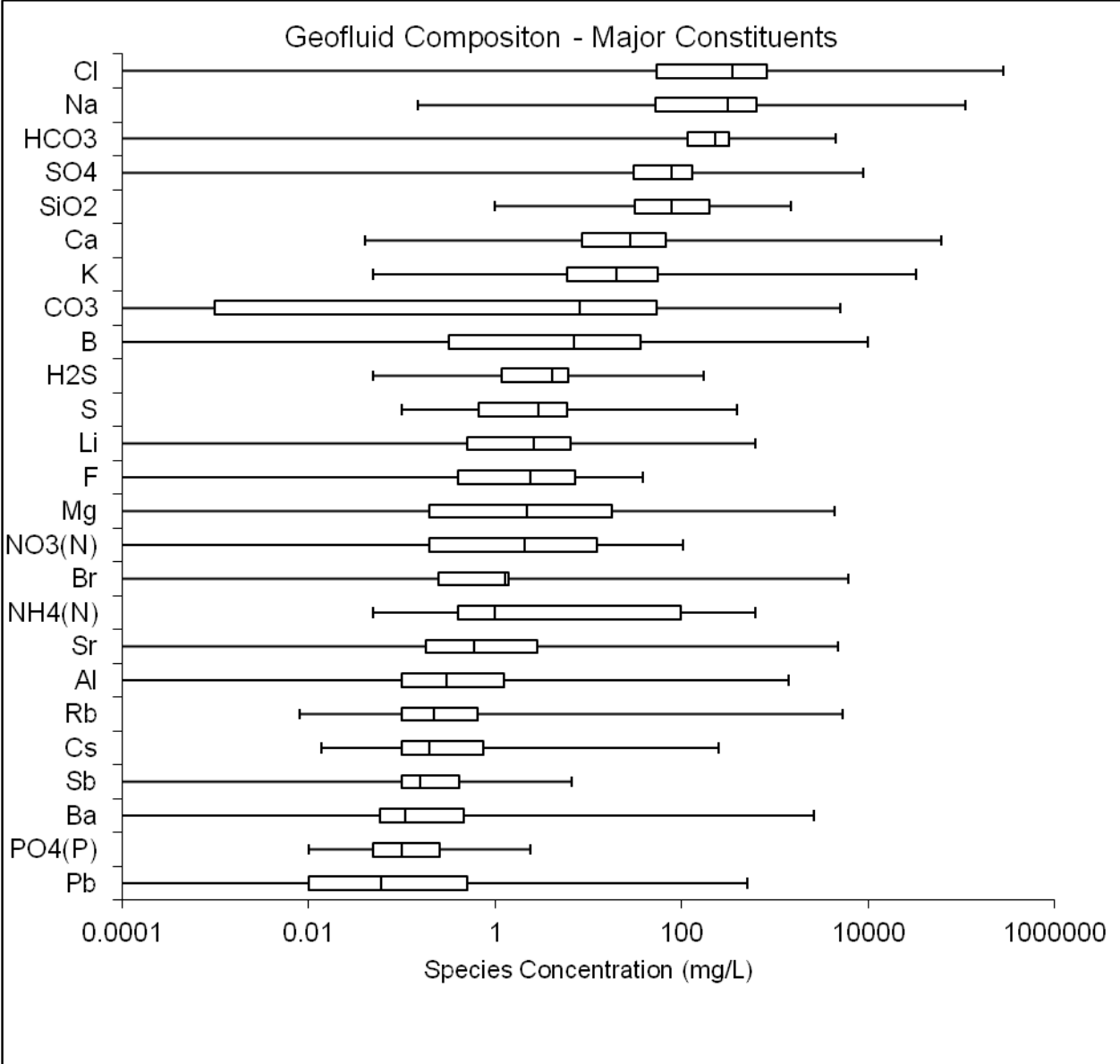


FIGURE 5-3 Geofluid Composition Box Plots, Major Constituents

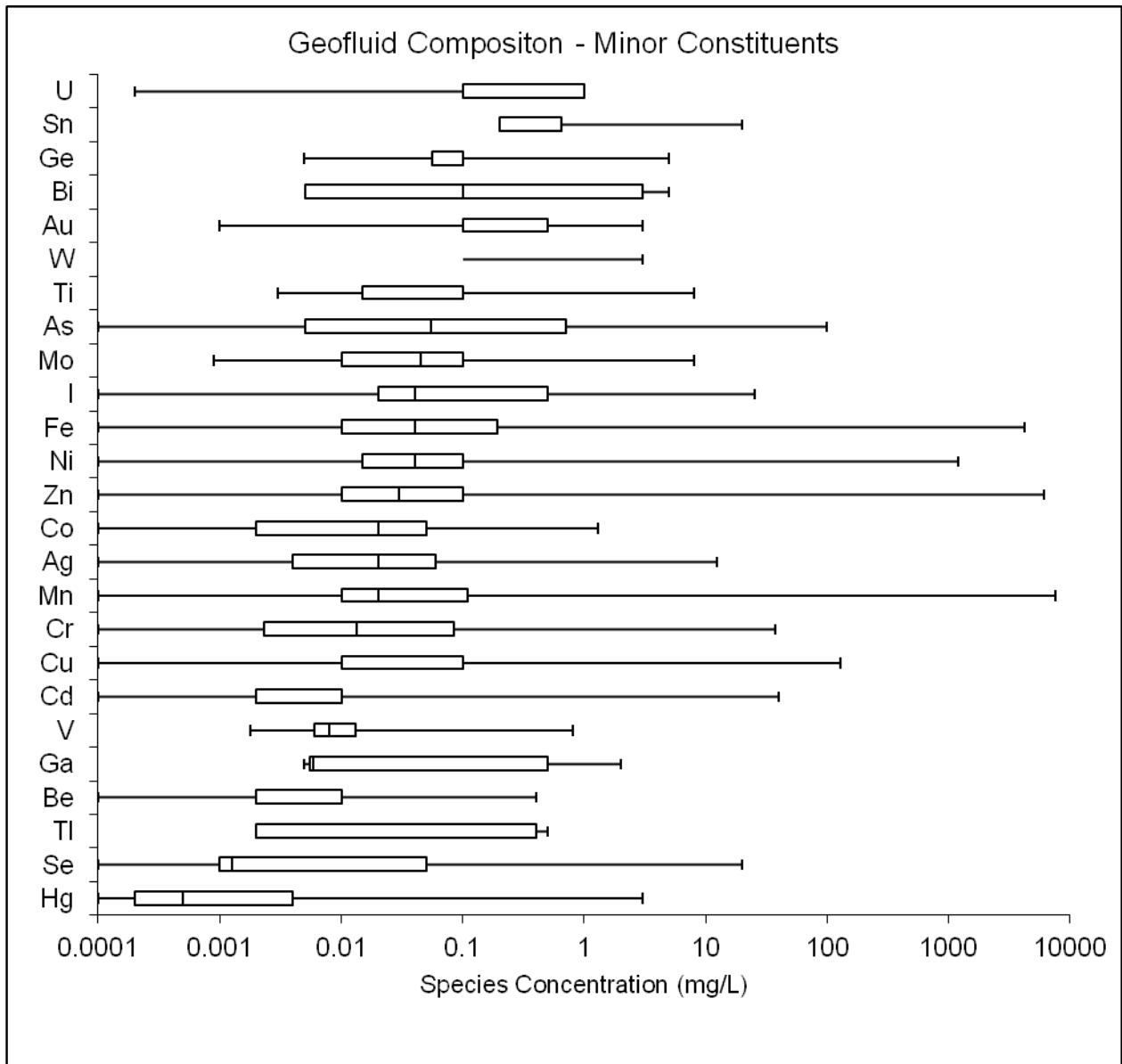
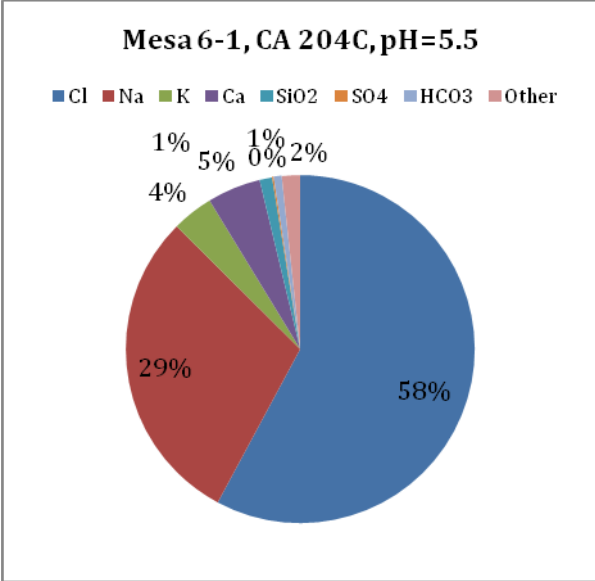
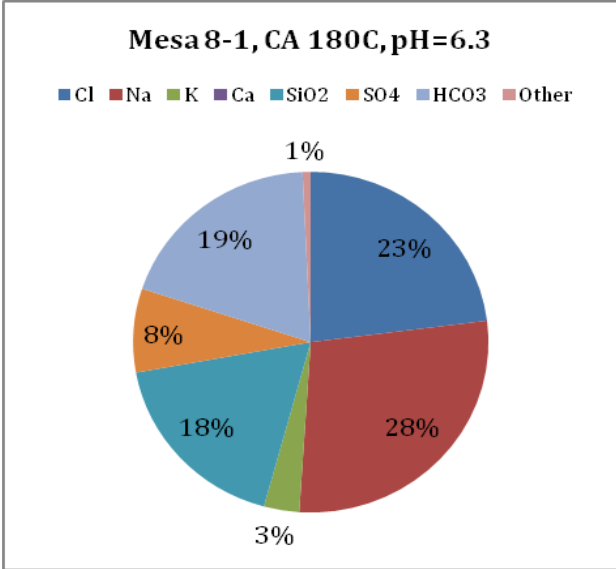


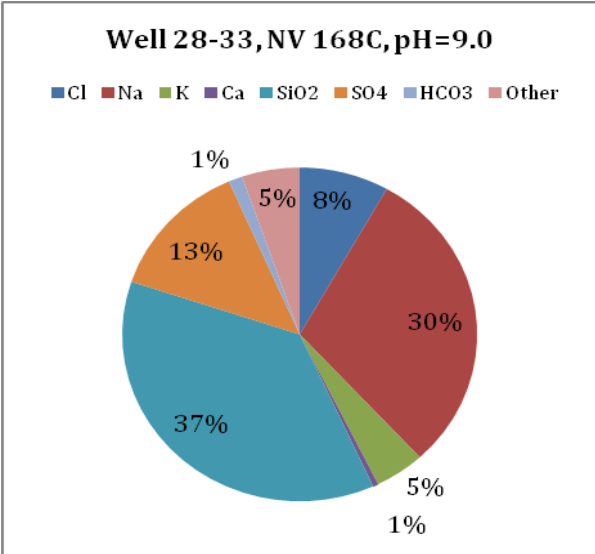
FIGURE 5-4 Geofluid Composition Box Plots, Minor Constituents



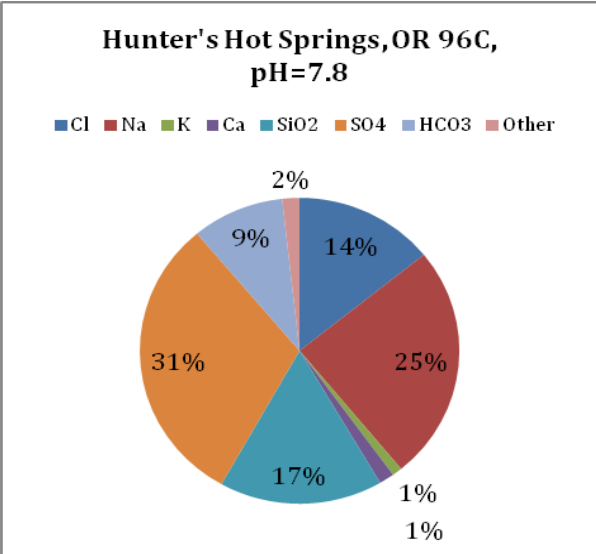
(a)



(b)



(c)



(d)

FIGURE 5-5 Geofluid Compositions of Selected Samples

TABLE 5-1 Comparison of Geofluid Composition with U.S. Primary Drinking Water Standards

| Constituent | High-Temperature Geofluids | | | | Moderate-Temperature Geofluids | | |
|---------------------|------------------------------|-----------------|------------------|----------------------------|--------------------------------|------------------|----------------------------|
| | Limit ^a (mg/L) | Mean (mg/L) | Median (mg/L) | Fraction meets standard | Mean (mg/L) | Median (mg/L) | Fraction meets standard |
| Antimony | 0.006 | 0.734 | 0.400 | 0.10 | 0.228 | 0.141 | 0.04 |
| Arsenic | 0.01 | 2.19 | 0.490 | 0.19 | 0.716 | 0.04 | 0.33 |
| Barium | 2 | 173 | 4.300 | 0.48 | 3.36 | 0.1 | 0.94 |
| Beryllium | 0.004 | 0.013 | 0.002 | 0.56 | 0.018 | 0.002 | 0.64 |
| Cadmium | 0.005 | 1.63 | 0.035 | 0.29 | 0.008 | 0.005 | 0.43 |
| Chromium | 0.1 | 1.033 | 0.030 | 0.55 | 0.012 | 0.006 | 1.00 |
| Copper ^b | 1.3 | 6.27 | 0.300 | 0.56 | 0.045 | 0.01 | 1.00 |
| Cyanide | 0.2 | ND ^c | ND | ND | ND | ND | ND |
| Fluoride | 4 | 4.13 | 2.50 | 0.75 | 4.98 | 2.39 | 0.59 |
| Lead ^b | 0.015 | 65.4 | 80.0 | 0.17 | 0.092 | 0.05 | 0.33 |
| Mercury | 0.002 | 0.192 | 0.005 | 0.29 | 0.005 | 0.0004 | 0.85 |
| Nitrate | 10 | 4.72 | 0.200 | 0.86 | 8.54 | 6.2 | 0.64 |
| Nitrite | 1 | ND | ND | ND | ND | ND | ND |
| Selenium | 0.05 | 0.790 | 0.055 | 0.50 | 0.015 | 0.001 | 0.88 |
| Thallium | 0.002 | ND | ND | ND | 0.219 | 0.1 | 0.00 |

^a All limits are maximum contaminant level (MCL) as defined by USEPA (2010)

^b Copper and lead are regulated based upon a specific treatment technology; above this limit additional treatment steps must be implemented.

^c ND indicates that there was no data for this chemical in this temperature range within the data set

TABLE 5-2 Comparison of Geofluid Composition with U.S. Secondary Drinking Water Standards

| Constituent | High-Temperature Geofluids | | | | Moderate-Temperature Geofluids | | |
|-------------|----------------------------|----------------|------------------|-------------------------------|--------------------------------|------------------|-------------------------------|
| | Limit (mg/L) | Mean (mg/L) | Median (mg/L) | Fraction Meets Standard | Mean (mg/L) | Median (mg/L) | Fraction Meets Standard |
| Aluminum | 0.2 | 73.2 | 1.00 | 0.28 | 13.9 | 0.223 | 0.40 |
| Chloride | 250 | 13259 | 166 | 0.66 | 2419 | 477 | 0.36 |
| Iron | 0.3 | 509 | 0.225 | 0.54 | 3.81 | 0.03 | 0.87 |
| Manganese | 0.05 | 467 | 0.050 | 0.48 | 6.59 | 0.02 | 0.74 |
| Silver | 0.1 | 0.974 | 0.060 | 0.50 | 0.027 | 0.02 | 0.98 |
| Sulfate | 250 | 156 | 108.000 | 0.91 | 173 | 72 | 0.88 |
| Zinc | 5 | 250 | 0.073 | 0.64 | 0.228 | 0.021 | 1.00 |
| TDS | 500 | 81077 | 2500 | 0.22 | 8226 | 1135 | 0.16 |
| pH | 6.5–8.5 | 6.51 | 6.40 | 0.42 | 7.63 | 7.5 | 0.66 |

The comparison with the drinking water standards clearly shows that there is a risk from the release of geofluids into drinking water, especially in terms of toxics such as antimony, arsenic, lead, and mercury. Although not universal, in general higher concentrations of contaminants were observed in the high-temperature than the moderate-temperature geofluids. It is important to note that this analysis is focused on geothermal sources likely to be used for utility-scale geothermal power production and is not necessarily applicable to shallow, low-temperature wells typically used for ground-source heat pumps.

5.3 NONCONDENSIBLE GASES

Geofluids always contain a fraction of dissolved noncondensable gases (NCG). Commonly encountered NCGs include nitrogen, carbon dioxide, hydrogen sulfide, methane, argon, and oxygen. These gases are released when steam is flashed and collect in the condenser of flash and steam systems. They must be removed to maintain efficient operation of the system. They are usually released to the atmosphere, except for hydrogen sulfide, which must be scrubbed prior to release.

Typical NCG concentrations range from 0.5% to 1.0% of the steam generated (DiPippo, 2008). Another data point indicates that NCG concentrations range from 0.2% to 1.8% of the steam produced from The Geysers geothermal field (Goldsmith, 1971). The release of NCG does not occur in binary systems because the gases remain dissolved in the pressurized geofluid and are reinjected into the reservoir. In the case of EGS, experience and data are limited, but it is expected that NCG volumes will be highly dependent upon the energy conversion approach taken (binary vs. flash), the properties of the reservoir, including any gases contained in the pore space, and the rate at which the fluid is circulated through the system. At present it appears that most EGS systems will use binary conversion systems, so the release of gasses will be limited to those that use flash or direct steam conversion.

Gas composition data were not included in the AGGD, but it was contained in a few of the component databases. Both the Mariner Database and the Great Basin Groundwater Geochemical Dataset contained some data on NCG composition (Mariner, 2010; GBCGE, 2010). The data in the Mariner Database were presented in terms of volume percent of the total NCG stream. Units for the gas composition data in the GBGGD were not indicated in the documentation. Personal communication with the database administrator indicated that the units were concentration units (mg/L) relative to the complete geofluid (Penfield, 2010). However, initial analysis of this data found some instances of mixed units being used (both mg/L and volume percent) for different records. Because of this uncertainty, only data from the Mariner Database were used.

Analysis of the data indicates that the composition NCG stream varies widely by location and is dominated by nitrogen and carbon dioxide. In most cases one or the other of these gases dominates the composition, but there are cases where the two gases are mixed more evenly. Concentrations of hydrogen sulfide, methane, oxygen, hydrogen, and argon are typically under 1% each but can reach as high as 10% in some cases. There is also a small subset of cases where

either hydrogen or methane dominates the composition with concentrations over 60%. Data on helium were also included in the dataset but is only present in trace amounts in most of the samples (typically under 0.1%).

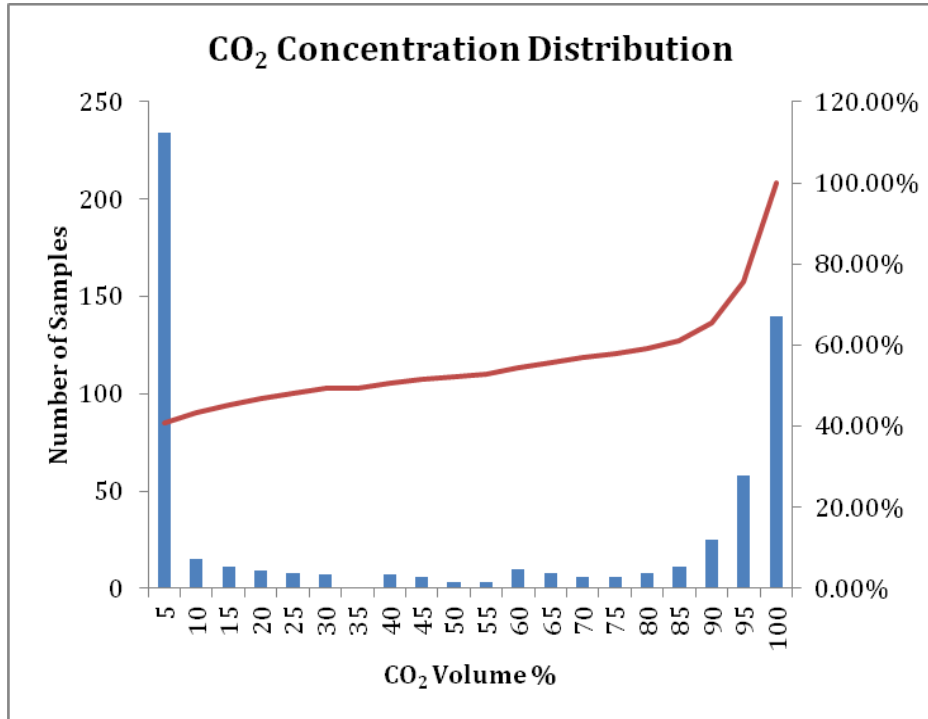


FIGURE 5-6 Histogram of Carbon Dioxide Concentrations in NCG Stream

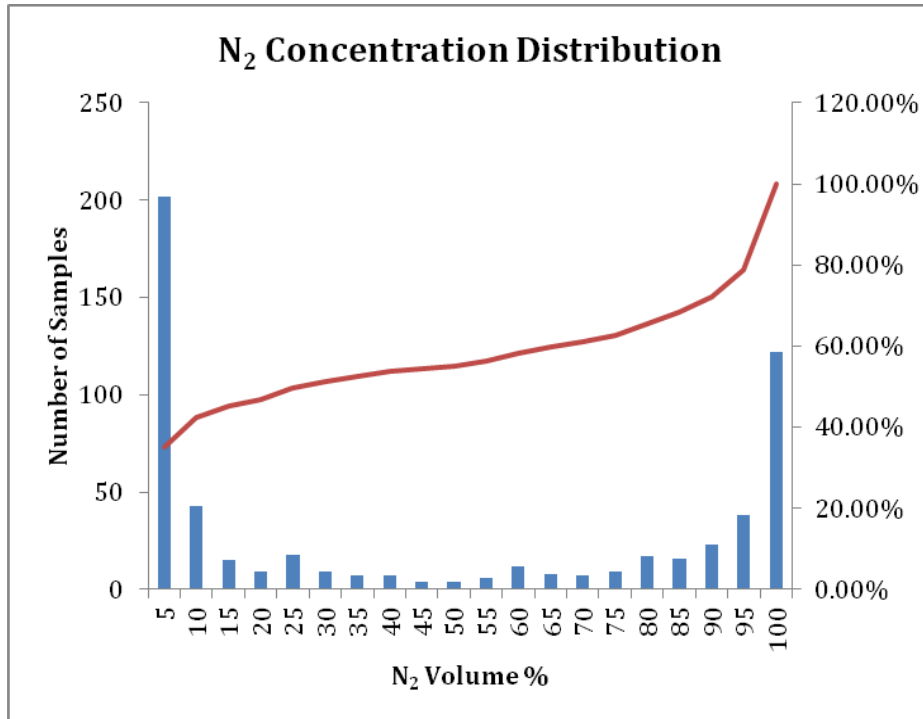


FIGURE 5-7 Histogram of Nitrogen Concentrations in NCG Stream

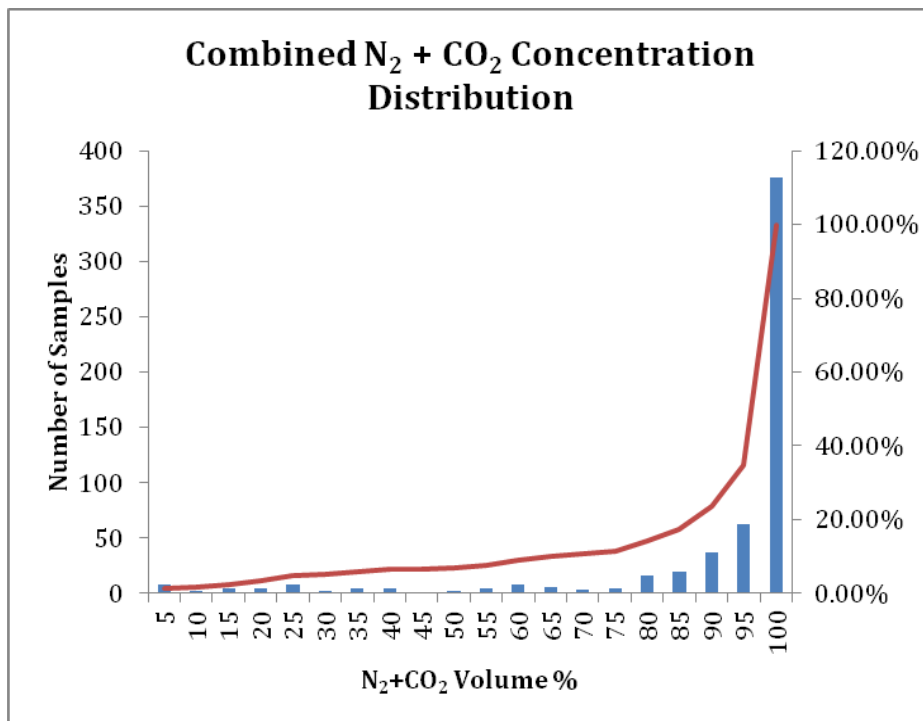
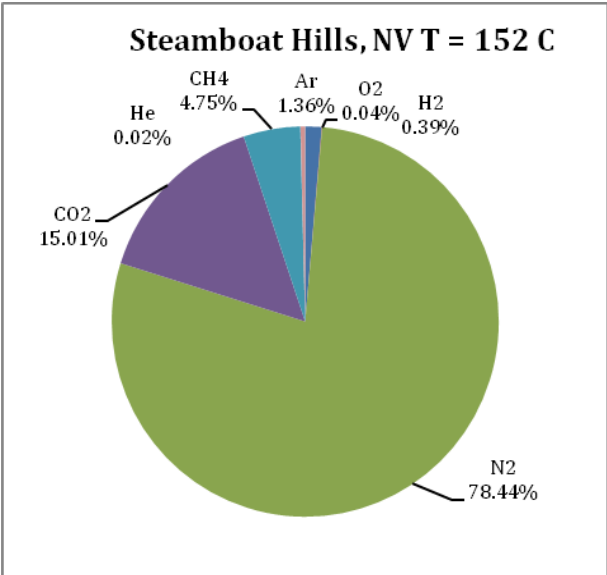


FIGURE 5-8 Histogram of Combined Nitrogen and Carbon Dioxide Concentrations in NCG Stream

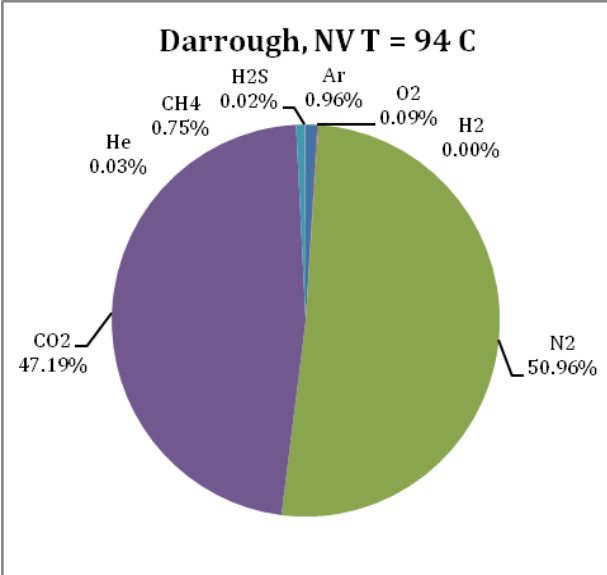
Figures 5-6 and 5-7 show the distribution of the concentrations of carbon dioxide and nitrogen, with the cumulative percentage for all of the samples on the right axis. The values on the x-axis are the upper end of the bin range (e.g., 5 represents the number of samples with a volume percentage from zero to 5%). The concentration distributions are almost identical for both gases, with most samples clustered over 90% or under 5%. In the case of carbon dioxide, 40% of samples had a concentration under 5% while another 40% had a concentration above 85%. In the case of nitrogen, 40% of the samples had a concentration under 10% while another 40% had a concentration above 70%.

Figure 5-8 better illustrates how nitrogen and carbon dioxide dominate the NCG composition. The combined concentration of these two gases is over 65% in 90% of samples and over 90% in 76% of samples. Figure 5-9 shows some examples of the complete composition of the NCG concentration of some geothermal resources. These samples were selected to show the variability in the concentrations. More examples can be found in Appendix D.

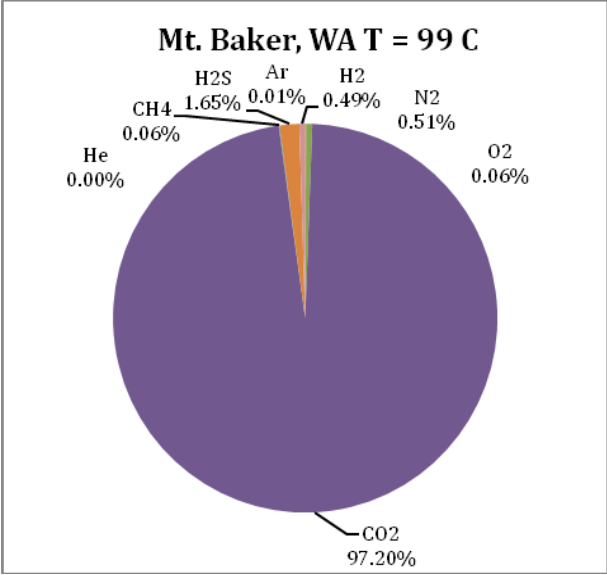
Variability in NCG composition is an important design consideration, at least for flash and steam systems. Increasing concerns over GHG emissions may require limiting emissions in the future. Compressing and reinjecting the NCGs into the reservoir with the spent geofluid is an option for limiting emissions from resources with higher CO₂ concentrations. This process, however, would result in additional parasitic power consumption (Tester et al., 2006). Targeting reservoirs with lower carbon dioxide concentrations is another option for limiting emissions. In addition to emissions concerns there are also locations with elevated hydrogen or methane concentrations. These gases could be separated and collected for use on site or sold into the market as an additional energy and revenue stream.



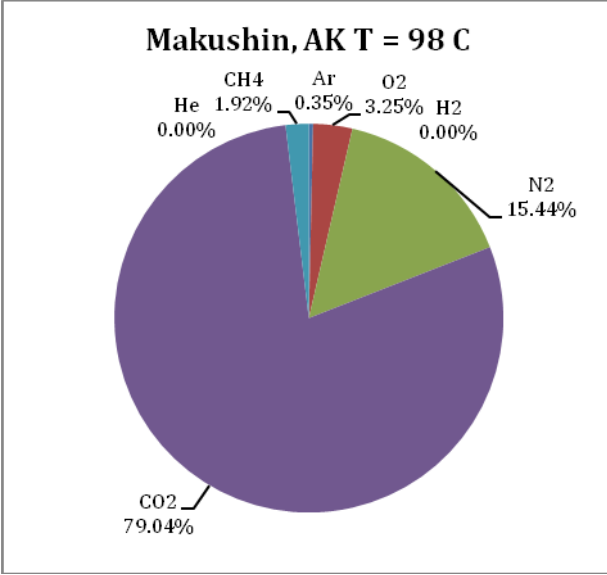
(a)



(b)



(c)



(d)

FIGURE 5-9 Examples of Noncondensable Gas Composition

5.4 SCALE FORMATION AND CORROSION

Geofluids are chemically complex and can result in extreme and harsh conditions that present difficult engineering challenges. Scale formation and corrosion are major operational considerations for geothermal plant design and operation. Both of these processes are directly related to the geofluid characteristics. Scale results from solids precipitating from the geofluid and attaching to the surfaces of pipes and equipment, whereas corrosion results from chemical interactions with the internal surfaces of process equipment.

Failure to properly manage corrosion and scale can result in restricted flow from production wells, reduced injectivity of injection wells, costly plant shutdowns, lower process efficiency, and equipment failure (Stapleton, 2002). Scale formation can produce an insulating effect, reducing the heat transfer coefficient to 30%–50% of the original value (Harley, 1973). This can be good for reducing thermal losses through transport pipes but bad for heat exchangers because it significantly reduces their effectiveness. Scale can also form a protective coating inside pipes, helping to inhibit corrosion (Harrar et al., 1979). Consequently, certain approaches taken to mitigate scale formation, such as acidification, may result in increased corrosion.

Scale formation within geothermal plants results from the precipitation of chemical species present in the geofluid. The three most common sources of scale in geothermal systems are metal sulfides, calcium carbonate (calcite), and silicon dioxide (silica) (Phillips et al., 1977). These different forms of scale typically impact different stages of the process, with sulfides and calcium carbonate usually precipitating early in the process and silica precipitating later, after the geofluid is concentrated through flashing or heat is removed in heat exchangers. Other minerals have also been known to contribute to scaling, including barite and fluorite (Harrar et al., 1979).

Metal sulfide scale formation is more complex and less understood than the other two forms of scale. A wide range of metals will precipitate as sulfides with different solubilities. In order of increasing solubility, these include: mercury, copper, lead, silver, iron, and zinc (Jackson and Hill, 1976). Sulfides of arsenic and antimony have also been observed (at the Salton Sea geothermal field) (Harrar et al., 1979). Sulfide scale formation is known to increase not just with decreasing temperature and increasing pH, but also under reduced (low-oxidation) conditions within the brine. Partial oxidation of brine or combined oxidation and acidification have been proposed as possible approaches for managing sulfide precipitation, but it is not clear whether either of these approaches has been tried on a pilot or commercial scale (Jackson and Hill, 1976). Alternatively, Weare and Moller (1989) suggest that metal sulfate scales are strongly controlled by dissolved hydrogen sulfate concentrations and are triggered by the release of gas from solution at the flash point. In general, most effort spent on controlling scale is targeted at calcite and silica, because their constituents are usually found in much higher concentrations in geothermal brines and there is less uncertainty in their formation mechanisms.

Compared with metal sulfide precipitation, calcium carbonate scale formation is a simpler process. Unlike metal sulfides and silica, calcite solubility increases as temperature decreases, thus the possibility of precipitation declines as energy is removed from the geofluid. The major driver of calcium carbonate scale formation is related to the concentration of

dissolved carbon dioxide. The removal of carbon dioxide from solution has two main influences on the likelihood of scale formation. The first is that it results in a sudden increase in pH, which favors the precipitate. The other is that the removal of carbon dioxide from solution drives the dissociation equilibrium toward the precipitate (DiPippo, 2008).

This unique mechanism for calcite scaling presents a major challenge for geothermal engineering. In many cases geofluids are allowed to flash within the wellbore at the natural flash horizon. If conditions are ripe for calcium carbonate scale formation (high calcium concentration, high dissolved carbon dioxide concentration) scale will begin to form at the flash horizon and can result in a constriction within the well bore, eventually choking off flow from the well. When left untreated, this process can result in the complete plugging of a well within days or weeks. This requires costly cleaning of the well bores and eventual replacement of well casing.

A method has been developed to prevent calcium carbonate scaling that involves continuous down-well injection of scale inhibitors, typically specialized and proprietary polymers. Scaling within the well bore can also be prevented through the use of downhole pumps to pressurize the fluid above the flash point. However, the thermodynamics of this method typically favor binary systems over flash systems (DiPippo, 2008).

In general, binary systems have fewer issues with calcium carbonate scaling because fluid is pressurized above the flash point throughout the process. However, calcium precipitates have been observed in some cases at locations where there is a pressure drop, such as across pumps (Wilson et al., 1978; Stapleton, 2002). It is hypothesized that pressure drops result in local evolution of carbon dioxide, which can temporarily create conditions conducive to calcite scale formation (Stapleton, 2002).

Silica is of greatest concern to most geothermal plants. Many geofluids leave their source in equilibrium with crystalline quartz. As the temperature of the geofluid decreases during energy production or the brine is concentrated through flashing of steam, the brine becomes more saturated with silica. One advantage is that the silica precipitates as amorphous silica, which has a higher solubility and allows for some concentration and cooling of the geofluid before precipitation occurs (Weare and Moller, 1989). This knowledge can be used in the design phase of a geothermal system to balance the tradeoff between maximum energy production and scale formation. It is usually easier to avoid scale formation in binary systems because only the temperature is being decreased and there is no concentration of the brine through the loss of geofluid to steam.

The amount of scale that forms is controlled by both solubility and kinetics. The rate of scale formation is strongly influenced by the pH: it is the most rapid in conditions of near-neutral pH and decreases in both acidic and basic brines. Silica scaling can thus potentially be controlled through modifying the pH. This approach may backfire in some cases, however, because the slowed precipitation may still occur in or around the injection well, impacting the permeability of the formation and reducing injectivity of the spent geofluid.

An alternative method of controlling silica scale is to induce precipitation through “seeding” of supersaturated fluid in a flash-crystallizer (DiPippo, 2008). Although generally of less concern than amorphous silica, silicon can also form complexes with various cations including iron, magnesium, calcium, and zinc (Stapleton, 2002). It has been suggested that controlling silica scale may reduce other forms of scale by acting as a substrate or nucleation site for other types of scale to form (Harrar et al., 1979).

The major drivers of scale formation and their mitigation options are summarized in Table 5-3. Arrows in the table indicate whether increasing or decreasing a driver will result in increased scaling.

Corrosion results from chemical interaction between the geofluid and the internal surfaces of equipment, including but not limited to well casing, pipes, and heat exchangers. It is a complex process and is dependent upon chloride concentration, pH, hydrogen sulfite partial pressure, and geofluid temperature (Phillips, 1977). Corrosion is typically managed through materials selection during the plant design process. Lining equipment with corrosion-resistant coatings or use of corrosion-resistant alloys are two common approaches. However, these materials are typically more costly than materials like carbon or lower-grade stainless steels. Since there is such wide variability in geofluids from location to location, it is recommended that materials are chosen only after testing them with the geofluid to be used.

TABLE 5-3 Summary of Geothermal Scale Formation Mechanisms and Mitigation Options

| Chemical Species | Drivers of Scale Formation | Mitigation Options |
|-----------------------------|--|---|
| Metal sulfide | ↓ Temperature, ↑ pH, ↓ oxidation state, ↓ dissolved H ₂ S | Oxidation of geofluid; Acidification of geofluid |
| Calcium carbonate (calcite) | ↑ Temperature, ↑ pH, ↓ dissolved CO ₂ | Pressurization of geofluid in the well bore; injection of specialized scale inhibitors |
| Silicon dioxide (silica) | ↓ Temperature, ↑ SiO ₂ concentration, pH close to neutral | Modification of system operating conditions to minimize oversaturation; modification of geofluid pH |

5.5 MINERAL EXTRACTION

In addition to energy production, geofluids have long been looked at as potential sources of other valuable resources, including minerals and freshwater. Between the 1960s and early 1980s there was significant interest in alternative or additional uses for geofluids; however, that interest seemed to die down throughout most of the 1980s and 1990s and has only recently been rekindled. As of 1982 there were no known operating commercial geothermal by-product production processes in the U.S. or worldwide (Lehr et al., 1982). It appears that this is still the case today. Interest in the area has grown in the last few years, with some pilot studies and proposed projects. A summary of the known by-product recovery projects and their history and status is presented in Table 5-4.

A significant advantage of mineral extraction from geofluids compared with other brines is that much of the difficult heavy lifting of well drilling and pumping are already done for energy production, lowering the bar for economic production. They are attractive largely due to the significant amount of mass that could be recovered; however, recovery is complicated by a number of factors, including low concentrations; complexity of the geofluids, which complicates extraction; and operational challenges such as scale and corrosion. The economics of mineral extraction are driven by geofluid chemistry, product quantity and quality, market price, market size and accessibility, and recovery cost (Lehr et al., 1982).

Historically much effort was focused on the production of potassium chloride (used for fertilizer production) and other salts, carbon dioxide for industrial purposes, and a range of industrial metals (e.g., zinc, lead, iron, magnesium, silver, manganese). None of these efforts proved economically viable over extended periods. Major challenges included high operating costs and changes in the market price of the product (Lehr et al., 1982; Blake, 1974). A recent venture attempted to extract zinc from the geofluid at the Salton Sea and ran into similar economic difficulty and was abandoned soon after it started (Salton Sea Funding, 2006). More recent efforts have focused on lithium and silica but it is too early to determine how successful they will be. In addition to minerals production, a number of efforts have also attempted to produce freshwater either directly from geofluids or to use geothermal energy as an energy source for desalination. These attempts have run into similarly challenging economics.

Lehr et al. (1982) present detailed descriptions of various separations processes that have been used or proposed for use to extract minerals from geothermal brines. Evaporation and crystallization was the preferred separation method in most previous mineral extraction processes. Requirements for reinjection of spent brine to preserve the resource and minimize subsidence severely limit its use in many current geothermal systems. Systems that utilize selective ion exchange or similar processes may have the most potential in these cases. Modern materials engineering may allow for the development of cheaper and more selective ion exchange resins that can better withstand the harsh conditions present in geofluids.

TABLE 5-4 Summary of Known Geothermal Byproduct Recovery Projects

| Location | Operator | Products | Scale | History/Status |
|---|--|--|--------------|--|
| Salton Sea, CA ^a | CalEnergy | Zn | Commercial | Operated for only a few years and shut down in 2004. Capital dismantled and sold off. |
| Wairakei geothermal system, New Zealand ^a | | Silica | Pilot | Operated for 11 months in the 1990s at pilot-scale but never put into production due to difficulty finding a buyer. |
| Mammoth Lakes, CA ^a ; and Imperial Valley, CA ^g | DOE, Lawrence Livermore National Lab., Simbol Mining | Silica, Li, Zn, Mn | Experimental | Started early 2000s, initial silica extraction technology is being used by Simbol Mining, which has received ARRA funds to develop experimental methods for extracting Li, Zn, and Mn from the Salton Sea. |
| Dixie Valley, NV; Coso, CA; and Steamboat Springs, NV ^a | DOE, Brookhaven National Lab. | Silica | Experimental | Work started in early 2000s, current status of the work is unknown. |
| Baja California, Mexico ^b | Pan American Lithium | Li | Proposed | Project still on the drawing board as of August 2010. |
| Kenya ^c | | CO ₂ for dry ice | Commercial | Reported in 1970s, unknown when production began or ended. |
| Larderello, Italy ^c | | H ₃ BO ₄ , NH ₃ , CO ₂ , H ₂ S, Borax | Commercial | Production began in 1930s and ended in 1971. The economics of borax production appears to have been the driving factor. |
| Cerro Prieto, Mexico ^c | | KCl | Pilot | Operated in the 1970s. |
| Salton Sea, CA (Magmax and Woolsley wells) ^c | U.S. Bureau of Mines, SRI International | Pb, Zn, Ag, Fe, Mn | Experimental | Program started in the late 1970s, unclear when it ended. |
| Raykjanes, Iceland ^c | | NaCl, KCl, CaCl ₂ | Feasibility | Process was designed in mid-1970s but it is unclear if it was ever built. |
| Danakil Depression, Ethiopia ^c | | Mg | Feasibility | Unknown whether it was ever studied further. |
| Imperial Valley, CA ^d | Shell Oil, Morton International | NaCl, KCl, CaCl ₂ | Commercial | Morton took over leases from Shell Oil and operated commercially from 1964 to 1967, focusing mainly on KCl production. The plant was dismantled soon after production stopped. |
| Imperial Valley, CA ^d | Union Oil Company | NaCl, KCl, CaCl ₂ | Pilot | Operated in the 1960s. Commercial-scale production never pursued due to scale and corrosion challenges and decline in product pricing. |
| Imperial Valley, CA ^c | U.S. Bureau of Mines, Hazen Research, WESTEC | Pb, Zn, Li, Fe, Mn, Al | Pilot | Operated a pilot plant but dismantled in early 1980s, shifted to concentrating on production of lithium toward the end of the program. |
| East Mesa, CA ^e | U.S. Bureau of Reclamation | Desalinated water | Pilot | A number of pilot-scale desalination units of different designs were installed and operated successfully throughout the 1970s. |
| New Mexico ^e | New Mexico State University | Desalinated water | Feasibility | Study performed in the last 1970s determined that desalination was not economically viable in New Mexico, even with the use of geothermal energy. |
| Kimolos, Greece ^f | European Geothermal Energy Council | Desalinated water | Pilot | Recent pilot study used a low-temperature geothermal (60°C–100°C) source to power a multistage distillation unit to produce high quality water. |

^a Bourcier et. al. (2003); ^b Pan American Lithium (2010); ^c Lehr et al. (1982); ^d Blake (1974); ^e Chaturvedi et al. (1979); ^f European Geothermal Energy Council (2007); ^g USDOE (2010).

Data on geofluid composition from the AGGD were used to perform some basic analyses of the economic potential of some example geothermal wells. An example is shown in Table 5-5 for a well within the East Mesa, California, geothermal field. Concentrations of a range of economically important minerals were multiplied by the known geofluid production rate of the entire field of 200,000 MT/day to determine a potential maximum annual production rate assuming 100% recovery (CDOGGR, 2009). The annual production potential was then multiplied by current 2010 prices for each substance to determine the potential market value. For the East Mesa field, the total calculated market value of minerals within the geofluid was just over \$90 million per year. In this case, the economic value was dominated by three products: potassium as potash, lithium, and silica. It is important to note that the price used for silica assumed high-purity silicon to be used for electronics production, which would require significant processing. Prices for lower-quality silica products are significantly lower and could decrease the market value by an order of magnitude.

This same calculation was repeated for five other data points in the AGGD. Each sample was selected due to high measured concentrations of one or more minerals and they are not expected to represent typical or average conditions. The flow rate in each of these cases was assumed to be the same as for the East Mesa field, which may not be realistic, but was selected to facilitate comparisons among wells. The results of this analysis are shown in Table 5-6. The total product value ranged from a few million to almost a billion dollars. The exact species that contributed the most to the economic potential varied significantly between wells also. Species that had resulted in economic potential above \$5 million in at least one location included silver, germanium, potassium, lithium, magnesium, manganese, nickel, selenium, silica, and zinc. Products with the greatest economic potential based upon this limited analysis are silver, potassium, lithium, manganese, silica, and zinc. This is consistent with the past history of geofluid mining. This history also shows, however, that large economic potential does not in any way guarantee that the resource can be exploited profitably.

TABLE 5-5 Analysis of Potential Revenue from Mineral Extraction at the East Mesa, CA, Geothermal Field

| Mineral | Price (\$/MT) | Concentration (mg/L) | Annual Production (MT/yr) | Market Value (\$/yr) |
|------------------|---------------|----------------------|---------------------------|----------------------|
| Ag | \$644,160 | 0.013 | 0.9 | \$611,308 |
| Co | \$37,400 | 0.06 | 4.4 | \$163,812 |
| Cu | \$7,436 | 0.1 | 7.3 | \$54,283 |
| Ge | \$900,000 | 0.1 | 7.3 | \$6,570,000 |
| K | \$351 | 1050 | 76,650 | \$26,896,485 |
| Li | \$6,600 | 40 | 2,920 | \$19,272,000 |
| Mg | \$3,163 | 17 | 1,241 | \$3,924,663 |
| Mn | \$2,860 | 0.95 | 69 | \$198,341 |
| Mo | \$31,350 | 0.005 | 0.4 | \$11,443 |
| Ni | \$21,736 | 0.1 | 7.3 | \$158,673 |
| Sb | \$10,120 | 5.5 | 402 | \$4,063,180 |
| Se | \$77,000 | 0.1 | 7.3 | \$562,100 |
| SiO ₂ | \$1,344 | 320 | 23,360 | \$31,400,512 |
| V | \$23,760 | 0.005 | 0.4 | \$8,672 |
| Zn | \$2,090 | 0.07 | 5.1 | \$10,680 |
| Total | | | | \$93,906,151 |

TABLE 5-6 Comparison of Economic Potential from Mineral Extraction of a Range of Geothermal Wells

| State | California | California | Nevada | Nevada | California | Utah |
|-------------------------|--------------------------------|----------------------------|--------------------|--------------------|-------------------------------------|---------------------------------------|
| Well Name | Hudson 1 – Magma Power Company | California State 2-14 well | D.F. 76-7 | Steamboat Springs | Mesa 6-1 U.S. Bureau of Reclamation | Phillips 3-1 – Phillips Petroleum Co. |
| Temperature (°C) | 180 | 298 | 163 | 91 | 204 | 205 |
| Ag | \$0 | \$98,749,728 | \$47,024 | \$2,821,421 | \$611,308 | \$0 |
| Co | \$0 | \$846,362 | \$5,460 | \$0 | \$163,812 | \$0 |
| Cu | \$3,256,968 | \$1,954,181 | \$13,571 | \$43,426 | \$54,283 | \$0 |
| Ge | \$0 | \$0 | \$0 | \$0 | \$6,570,000 | \$0 |
| K | \$532,806,560 | \$368,866,080 | \$26,384 | \$1,383,248 | \$26,896,485 | \$11,475,834 |
| Li | \$153,694,200 | \$105,996,000 | \$4,818 | \$3,661,680 | \$19,272,000 | \$9,636,000 |
| Mg | \$5,771,563 | \$8,311,050 | \$2,309 | \$46,173 | \$3,924,663 | \$2,309 |
| Mn | \$271,414,000 | \$250,536,000 | \$3,340 | \$4,176 | \$198,341 | \$0 |
| Mo | \$0 | \$2,288,550 | \$22,886 | \$228,855 | \$11,443 | \$0 |
| Ni | \$0 | \$9,599,704 | \$5,950,230 | \$23,801 | \$158,673 | \$0 |
| Sb | \$0 | \$738,760 | \$813 | \$0 | \$4,063,180 | \$0 |
| Se | \$0 | \$5,621,000 | \$562 | \$281,050 | \$562,100 | \$0 |
| Si | \$0 | \$10,892,053 | \$451,480 | \$0 | \$31,400,512 | \$54,950,896 |
| V | \$0 | \$0 | \$3,469 | \$520,344 | \$8,672 | \$0 |
| Zn | \$0 | \$73,996,450 | \$10,680 | \$3,051 | \$10,680 | \$0 |
| Total | \$966,943,291 | \$938,395,918 | \$6,543,026 | \$9,017,224 | \$93,906,151 | \$76,065,038 |

6 SUMMARY AND CONCLUSIONS

This report presents a comprehensive and comparative LCA of water consumption for large-scale geothermal power plant systems. Geothermal power plants consume less water per kilowatt-hour of lifetime energy output than other electric power generation technologies. Flash power plants consume the least amount of water (0.006–0.01 gal/kWh) due to their reliance on geofluid for cooling, although the long-term sustainability of such an approach is unknown with average geofluid losses estimated at 2.7 gal/kWh. For binary systems, only wind and photovoltaic electric power systems reportedly consume less water. This study estimates that binary systems consume 0.27 gal/kWh, although literature estimates report cooling consumption as low as 0.15 gal/kWh. EGS power plants have similar water consumption rates to NGCC and biomass power plants, although the water use for biomass power plants is likely to be higher than estimated because fuel production water requirements were not included in our analysis.

This LCA found the water consumption for EGS power plants to be 0.30–0.72 gal/kWh over the lifetime energy output. These findings are similar to those reported in Frick et al. (2010), who provided component estimates of consumption that aggregate to 0.36 gal/kWh over the lifetime energy output. However, Frick et al. (2010) identified the construction stage, particularly well stimulation or “reservoir enhancement,” as the stage where most of the water is consumed. While stimulation dominated the construction stage volume requirements in this LCA, over the lifetime energy output the volume for the entire construction stage is 0.01 gal/kWh for EGS. It is unclear why there is such a large difference; however if “reservoir enhancement” includes additional makeup water over time due to water loss, Frick et al.’s operation water loss results are similar to this LCA’s.

For all geothermal systems evaluated, the operational makeup water requirement was found to be the largest consumer of water. The operation water losses for the binary and EGS scenarios were based on available data for operating air-cooled systems, although the data are likely high due to evaporative cooling operations during the daytime during summer months. An air-cooled plant without a hybrid cooling system would likely have lower consumption values than those reported here.

While operational water losses for air-cooled systems may be overestimated in the EGS scenarios, potential subsurface water losses from reservoir stimulation are not accounted for. Insufficient empirical data exists to support a reservoir water loss estimate; further research may support a reasonable estimate in the future.

Comparison of the geofluid composition with U.S. drinking water standards concluded that geothermal waters pose a large potential risk to water quality, if released into the environment, due to high concentrations of toxics including antimony, arsenic, lead, and mercury. However, the risk of release can be virtually eliminated through proper design and engineering controls. The potential for mineral extraction from the geofluid was evaluated and it was concluded that while the market value of the minerals contained in some geofluids can be very high in some cases, the economics of extraction have proved to be quite challenging

historically. It is unclear at this time whether new technology and materials will allow profitable exploitation of these resources going forward.

The results of this LCA lead to the following recommendations to reduce the life cycle water intensity or improve operations of geothermal power plants.

1. **Reuse water.** Reusing water during construction can reduce the estimated volume of water for these activities. Drilling muds and hydraulic stimulation fluids are often reused when feasible. When multiple wells are drilled or stimulated on a site, temporarily storing fluids between activities could reduce overall water volumes.
2. **Evaluate operational water use.** For all geothermal systems evaluated, operational water consumption was the most significant contributor to water consumption over the life cycle. There is a lack of available data to identify where water consumption is occurring during operations, especially for air-cooled systems. Further evaluation could identify processes that are consuming water and possibly present opportunities for improving operational water use efficiency.
3. **Consider nonfreshwater makeup sources.** If water availability is limited or there are several competing users for a single source, shifting water consumption to nonfreshwater sources when feasible may be an effective solution to water consumption concerns. Alternative sources include oil and gas production water, carbon capture and storage production water, and saline groundwater.
4. **Encourage use of binary systems.** Binary systems were found to mitigate or minimize some of the major environmental and operational impacts resulting from the geofluid composition. They eliminate the venting of NCG, reducing the carbon footprint and the need for hydrogen sulfide controls. They minimize or eliminate many of the key drivers of scale formation. Binary systems also enhance the sustainability of the reservoir by avoiding geofluid evaporative cooling losses.

Through these efforts, efficiency improvements can be made across the geothermal power plant life cycle to further reduce the impacts of geothermal power on freshwater resources.

7 REFERENCES

- Adee, S., and S.K. Moore, 2010, "In the American Southwest, the Energy Problem Is Water," *IEEE Spectrum*, available at <http://spectrum.ieee.org/environment/in-the-american-southwest-the-energy-problem-is-water>, June.
- Asanuma, H., Y. Kumano, T. Izumi, N. Soma, H. Kaieda, K. Tezuka, D. Wyborn, and H. Niitsuma, 2004, "Passive Seismic Monitoring of a Stimulation of HDR Geothermal Reservoir at Cooper Basin, Australia," *Technical Program Expanded Abstracts* 23:556-559, Society of Exploration Geophysicists.
- Blake, R.L., 1974, "Extracting Minerals from Geothermal Brines: A Literature Study," Twin Cities Metallurgy Research Center, Twin Cities, MN, prepared for U.S. Department of the Interior, Bureau of Mines.
- Bourcier, W.L., M. Lin, and G. Nix, 2005, "Recovery of Minerals and Metals from Geothermal Fluids," presented at the 2003 SME Annual Conference, Cincinnati, OH, February 24-26, available at <https://e-reports-ext.llnl.gov/pdf/324646.pdf>.
- Boustead, I., and Hancock, G.F., *Handbook of Industrial Energy Analysis*, Halsted Press, John Wiley & Sons, 1979.
- California Division of Oil, Gas, and Geothermal Resources (CDOGGR), 2009, "Summary of Geothermal Operations," *The Preliminary 2008 Annual Report of California Oil, Gas and Geothermal Production*, available at ftp://ftp.consrv.ca.gov/pub/oil/annual_reports/2008/0109geofin_08.pdf.
- Campbell, R., 2000, "Mammoth Geothermal – A Development History," *GRC Bulletin*, pp 91-95, May/June.
- Chatervendi, L., C.G. Keyes Jr., C.A. Swanberg, Y.P. Gupta, 1979, "Use of Geothermal Energy for Desalination in New Mexico — A Feasibility Study," New Mexico State University, Las Cruces, NM, prepared for the New Mexico Energy and Minerals Department.
- Culver, G., and K.D. Rafferty, 1998, "Well Pumps," *Geothermal Heat Center Bulletin*, pp. 7-10, March.
- DiPippo, R., 2008, *Geothermal Power Plants, Second Edition: Principles, Applications, Case Studies, and Environmental Impact*, Butterworth-Heinemann, Elsevier.
- Duffield, W.A., and J.H. Sass, 2003, "Geothermal Energy — Clean Power From the Earth's Heat," *U.S. Geological Survey Circular 1249*, available at <http://pubs.usgs.gov/circ/2004/c1249/c1249.pdf>.

European Geothermal Energy Council, 2007, “Geothermal Desalination,” available at <http://www.egec.org/target/Brochure%20DESALINATION.pdf>.

E-Z Line Pipe Support Co., LLC, 2005, “Foundation Detail for Pipe Support Figure 510: 16-inch Diameter,” Manvel, TX.

Frick, S., M. Kaltschmitt, and G. Schröder, 2010, “Life Cycle Assessment of Geothermal Binary Power Plants Using Enhanced Low-Temperature Reservoirs,” *Energy* 35: 2281-2294.

Garside, L., 1994, “Nevada Low-Temperature Resource Assessment,” Nevada Bureau of Mines and Geology, Reno, NV, available at <http://www.nbmgs.unr.edu/dox/of942.htm>.

Gleick, P.H., 1992, “Environmental Consequences of Hydroelectric Development — the Role of Facility Size and Type,” *Energy* 17(8), 735-747.

Gleick, P.H., 1994, “Water and Energy,” *Ann. Rev. Energy Environ.* 19, 267-299.

Goldsmith, M., 1971, “Geothermal Resources in California: Potentials and Problems,” California Institute of Technology, Environmental Quality Laboratory, Pasadena, CA, available at <http://caltecheql.library.caltech.edu/14/>.

Goldstein, R., and W. Smith, 2002, *Water & Sustainability (Volume 3): U.S. Water Consumption for Power Production — The Next Half Century*, EPRI 1006786, available at <http://mydocs.epri.com/docs/public/000000000001006786.pdf>, March.

Great Basin Center for Geothermal Energy (GBCGE), 2010, Great Basin Groundwater Geochemical Database, available at <http://www.unr.edu/geothermal/geochemDB.htm>.

Halliburton, Inc., 2006. “API Class G Cement: Slurry Properties,” eRedbook Software, available at <http://www.halliburton.com/ps/default.aspx?navid=184&pageid=663&prodid=PRN::IYFX5Y2B7>.

Halliburton, Inc., 2008, “Quick-Gel Gold,” available at http://www.baroididp.com/public_idp/products-apps/pubsdata/Data_Sheets/I_Z/QUIK-GEL_GOLD.pdf.

Harley, P.H., 1973, “SiO₂ Scale Formation in Simulated Geothermal Brine,” Oak Ridge National Laboratory, Oak Ridge, TN, prepared for Department of the Interior, Office of Saline Water.

Harrar, J.E., C.H. Otto, Jr., S.B. Deutscher, R.W. Ryon, and G.E. Tardiff, 1979, “Studies of Brine Chemistry, Precipitation of Solids, and Scale Formation at the Salton Sea Geothermal Field,” Lawrence Livermore National Laboratory, Livermore, CA.

Harto, C., R. Meyers, and E. Williams, 2010, “Life Cycle Water Use of Low-Carbon Transport Fuels,” *Energy Policy* 38:4933-4944.

Illinois Department of Transportation, 2007, “Section 1019: Controlled Low-Strength Material (CLSM),” *Standard Specifications for Road and Bridge Construction*, pp. 758-760.

Jackson, D., and J.H. Hill, 1976, “Possibilities for Controlling Heavy Metal Sulfides in Scale from Geothermal Brines,” Lawrence Livermore National Laboratory, Livermore, CA.

Lehr, L., A.D. Allen, and R. Lease, 1982, “Potential for By-Product Recovery in Geothermal Energy Operations,” Energy and Economics Research Inc, Vienna, VA, prepared for Geothermal and Hydropower Division, U.S. Department of Energy.

Mansure, A.J., 2010, “Review of Past Geothermal Energy Return on Investment Analyses,” *GRC Transactions*, Geothermal Resources Council, Davis, CA.

Mariner, R.H., 2010, personal communication between Robert Mariner, U.S. Geological Survey, Menlo Park, CA, and Christopher Harto, Argonne National Laboratory, Washington, DC, April 2.

Maulbetsch, J.S., and M.N. DiFilippo, 2006, “Cost and Value of Water Use at Combined-Cycle Power Plants,” Pier Final Project Report, CEC-500-2006-034, prepared for California Energy Commission, Public Interest Energy Research.

McAllister, E.W., 2009, “Spacing of Pipe Supports,” *Pipeline Rules of Thumb Handbook*, 7th Edition, Gulf Professional Publishing, Houston, TX.

Michelet, S., and M.N. Toksöz, 2006, “Fracture Mapping in the Soultz-sous-Forêts Geothermal Field from Microearthquake Relocation,” Earth Resources Laboratory Consortium Report, available at <http://www-eaps.mit.edu/erl/research/report1/pdf2006/Michelet06.pdf>.

Moore, M., 2010, personal communication between Melissa Moore, Kansas Geological Survey, Lawrence, KS, and Christopher Harto, Argonne National Laboratory, Washington, DC, March 8.

Narasimhan, T.N., and P.A. Witherspoon, 1977, “Reservation Evaluation Tests on RRG 1 and RRG2, Raft River Geothermal Project, Idaho,” Lawrence Berkeley Laboratory, Berkeley, CA, available at <http://www.osti.gov/bridge/servlets/purl/7305201-Rik8v4/7305201.pdf>.

National Energy Technology Laboratory (NETL), 2005, “Power Plant Water Usage and Loss Study,” U.S. Department of Energy, National Energy Technology Laboratory, available at http://www.netl.doe.gov/technologies/coalpower/gasification/pubs/pdf/WaterReport_Revised%20May2007.pdf, revised May 2007.

NETL, 2007, “Estimating Freshwater Needs to Meet Future Thermoelectric Generation Requirements, 2007 Update,” DOE/NETL-400/2007/1304, available at http://www.fypower.org/pdf/DOE_WaterNeedsAnalysis_2007.pdf, September 24.

Pan American Lithium Corp., 2010, “Mexican Geothermal Lithium Project,” available at <http://www.panamericallithium.com/chilean-salar-brine-project/test>.

Penfield, R., 2010, personal communication between Robin Penfield, Great Basin Center for Geothermal Energy, Reno, NV, and Christopher Harto, Argonne National Laboratory, Washington, DC, April 29.

Phillips, S.L., A.K. Mathur, and R.E. Doebler, 1977, “A Study of Treatment Methods for Geothermal Fluids,” presented at the SPE International Symposium on Oilfield and Geothermal Chemistry, University of California, San Diego, June 27–29, available at <http://www.osti.gov/bridge/purl.cover.jsp;jsessionid=76B484B703DB5395B054688F2E51FA71?purl=/7318047-m912TA/>.

Radback Energy, 2009, “Appendix 5.1E Construction Data, Contra Costa Generating Station — Application for Certification,” Docket 09-AFC-4, The California Energy Commission, available at http://www.energy.ca.gov/sitingcases/oakley/documents/applicant/afc/Volume%202/CCGS_Appendix%205.1E_Construction%20Data.pdf.

Salton Sea Funding, 2006, “Combined Financial Statements as of December 31, 2005, and 2004 and for Each of the Three Years in the Period Ended December 31, 2005,” available at: http://www.midamerican.com/include/pdf/sec/20051231_49_ssf_annual.pdf.

Smith, D.J., 2002, “Evaporative Cooling Increases Summer Capacity at Geothermal Plant,” *Power Engineering* 106(2), available at <http://www.powergenworldwide.com/index/display/articledisplay/137080/articles/power-engineering/volume-106/issue-2/field-notes/evaporative-cooling-increases-summer-capacity-at-geothermal-plant.html>.

Sonoco Products Company, 2008, “Sonotube Concrete Forms,” technical leaflet, http://sonotube.com/europe/docs/IPDEuro_techsheets_ENG.pdf.

Stapleton, M., 2002, “Scaling and Corrosion in Geothermal Operation,” PowerChem Technology, Minden, NV.

Sullivan, J.L., C.E. Clark, J.W. Han, and M.Q. Wang, 2010, “Life Cycle Analysis Results of Geothermal Systems in Comparison to Other Power Systems,” Argonne Technical Report, ANL/ESD/10-5, available at <http://www.ipd.anl.gov/anlpubs/2010/09/67933.pdf>.

Tester, J.W., et al. (2006), “The Future of Geothermal Energy: Impact of Enhanced Geothermal Systems (EGS) on the United States in the 21st Century,” Massachusetts Institute of Technology, available at http://geothermal.inel.gov/publications/future_of_geothermal_energy.pdf.

Tonnessen, K., 1975, “Environmental Aspects of Geothermal Energy Development: Salton Sea/Imperial Valley Area,” Lawrence Livermore National Laboratory, University of California, Livermore, CA.

U.S. Department of Energy (USDOE), 2010, “Technologies for Extracting Valuable Metals and Compounds from Geothermal Fluids,” available at <http://www1.eere.energy.gov/geothermal/projects/projects.cfm/ProjectID/169>.

U.S. Department of Interior (USDOI) and U.S. Department of Agriculture (USDA), 2008, “Programmatic Environmental Impact Statement for Geothermal Leasing in the Western United States,” FES 08-44, available at http://www.blm.gov/wo/st/en/prog/energy/geothermal/geothermal_nationwide/Documents/Final_PEIS.html.

U.S. Environmental Protection Agency (USEPA), 2010, “Drinking Water Contaminants,” Web site, available at <http://www.epa.gov/safewater/contaminants/index.html>.

U.S. Geological Survey (USGS), 1983, GOETHERM Database, available at <http://www.nbmng.unr.edu/geothermal/geochemdata/geotherm.htm>, accessed March 4, 2010.

U.S. Geological Survey (USGS), 2006, Chemical and Isotope Data, database available at <http://hotspringchem.wr.usgs.gov/>, accessed March 25, 2010.

U.S. Government Accountability Office (GAO), 2009, “Energy-Water Nexus, Improvements to Federal Water Use Data Would Increase Understanding of Trends in Power Plant Water Use,” Report to the Chairman, Committee on Science and Technology, House of Representatives, GAO-10-23, October.

Vestas Wind Systems A/S, 2006, “Life Cycle Assessment of Electricity Produced from Onshore Sited Wind Power Plants based on Vestas V82-1.65 MW Turbines,” available at <http://www.vestas.com/Admin/Public/DWSDownload.aspx?File=%2FFiles%2FFiler%2FEN%2FSustainability%2FLCA%2FLCAV82165MWonshore.pdf>, accessed August 2010.

Weare, J.H., and N.E. Moller, 1989, “Prediction of Scaling in Geothermal Systems,” *Proceedings of the Geothermal Program Review VII, DOE Research and Development for the Geothermal Marketplace*, San Francisco, CA, March 21-23, available at <http://www.osti.gov/geothermal/servlets/purl/890490-bEqSln/890490.pdf>.

Wilson, J.S., J.E. King, and G.R. Bullard, 1978, “Study on Scale Formation and Suppression in Heat-Exchanger Systems for Simulated Geothermal Brines,” The Dow Chemical Company, Texas Division, Freeport, TX, prepared for the U.S. Department of Energy, Geothermal Energy.

Zimmermann, G., I. Moeck, and G. Blocher, 2009, Cyclic Waterfrac Stimulation to Develop an Enhanced Geothermal System (EGS) — Conceptual Design and Experimental Results, *Geothermics* 39(1):59-69, March.

APPENDIX A – ARGONNE GEOTHERMAL GEOCHEMICAL DATABASE

This appendix describes what is contained within the Argonne Geothermal Geochemical Database (AGGD), including the format and units. The database is organized into an Excel spreadsheet with five pages and can be downloaded at <http://www.anl.gov/renewables/research/geothermal.html>. The first page describes the data sources and assigns a number code to each source for identification of entries within the database. The second page contains all the data entries within the database regardless of temperature. The third page contains only those entries with a defined temperature above 90°C. The fourth page contains only those entries with a defined temperature between 90 and 150°C, or moderate temperature geothermal sources as defined by the USGS. The fifth page contains only those entries with a defined temperature above 150°C, or high temperature geothermal sources as defined by the USGS. All data, regardless of the page, are in the exact same format, with the following fields:

- **Data Source** – Gives a number code for the original source of the data entry
- **Name** – Name given to the sampling location by the original source
- **Date** – Date when the original sample was taken
- **Longitude** – Longitude in decimal format
- **Latitude** – Latitude in decimal format
- **State** – The state where the sampling location is located
- **Depth** – ft – The depth from which the sample was obtained in feet
- **Temp** – C – The temperature of the sample in degrees Celsius
- **pH** – The pH of the sample
- **TDS** – mg/L – Total dissolved solids in milligrams per liter
- **Xx** – mg/L – The concentration of the specific chemical constituent Xx in milligrams per liter

The chemical constituents in the database are:

| | | | | | | | | |
|----|----|----|------------------|---------------------|----|---------------------|-----------------|---------------------|
| Ag | Al | As | Au | B | Ba | Be | Bi | Br |
| Ca | Cd | Cl | Co | CO ₃ | Cr | Cs | Cu | F |
| Fe | Ga | Ge | H ₂ S | HCO ₃ | Hg | I | K | Li |
| Mg | Mn | Mo | Na | NH ₄ (N) | Ni | NO ₃ (N) | Pb | PO ₄ (P) |
| Rb | S | Sb | Se | SiO ₂ | Sn | SO ₃ | SO ₄ | Sr |
| Th | Ti | Tl | U | V | W | Zn | | |

APPENDIX B – DETAILED LIFE CYCLE INVENTORY DATA

Additional quantitative data on the life cycle inventory are included in this appendix. Table B-1 provides the process-based inventory data aggregated for the four geothermal scenarios considered in this study. Table B-2 compares the total life cycle water use per lifetime energy output found in this study with values found in the literature for geothermal and other electric power generation technologies.

TABLE B-1 Water Use by Life Cycle Stage. Uncertainty in the well construction stage accounts for variations in flow rates, downhole temperatures, and other parameters that affect the total number of wells required to generate a set amount of power. Uncertainty for the EGS scenarios is based on available binary replacement and loss data from CDOGGR (2010).

| Construction Stages | Scenario Water Use in Gallons | | | |
|--|----------------------------------|----------------------------------|------------------------|---------------------------|
| | 20-MW EGS | 50-MW EGS | 10-MW Binary | 50-MW Flash |
| Well construction by depth (km) | | | | |
| 0.67 ^a | | | 1,085,000 ± 256,000 | |
| 1 ^a | | | 1,412,000 ± 326,000 | |
| 1.5 ^a | | | 1,841,000 ± 415,000 | 7,755,000 ± 2,356,000 |
| 2 ^a | | | 2,239,000 ± 488,000 | 9,726,000 ± 2,921,000 |
| 2 ^b | | | | 14,554,000 ± 4,372,000 |
| 2.5 ^b | | | | 18,714,000 ± 5,604,000 |
| 3 ^b | | | | 21,003,000 ± 6,269,000 |
| 4 ^c | 8,164,000 ± 4,159,000 | 20,346,000 ± 10,381,000 | | |
| 5 ^c | 9,699,000 ± 5,087,000 | 24,196,000 ± 12,732,000 | | |
| 5 ^d | 14,131,000 ± 7,412,000 | 35,255,000 ± 18,551,000 | | |
| 6 ^d | 16,051,000 ± 8,792,000 | 40,068,000 ± 22,000,000 | | |
| 6 ^e | 28,858,000 ± 15,807,000 | 72,040,000 ± 39,555,000 | | |
| Stimulation | 38,745,000 | 96,646,000 | | |
| Surface Piping | 39,000 | 98,000 | 18,000 | 90,000 |
| Plant Construction | 214,000 | 536,000 | 107,000 | 182,000 |
| Plant Operations | 2,663,645,250 ± 1,141,562,250 | 6,644,260,669 ± 2,847,540,287 | 1,068,082,402 | 76,544,146 |

^a Based on Raft River wells (Narasimhan and Witherspoon, 1977). This design does not include an intermediate liner.

^b Based on Raft River wells (Narasimhan and Witherspoon, 1977). This design includes an intermediate liner.

^c Based on Tester et al. (2006). This design has one liner and two casings.

^d Based on Tester et al. (2006). This design has two liners and two casings.

^e Based on Tester et al. (2006). This design has three liners and two casings.

TABLE B-2 Water Consumption where Significant for Electric Power Generation at Indicated Life Cycle Stages — in Gallons per Kilowatt-Hour of Lifetime Energy Output

| Life Cycle Stage | Cooling System Type | | | Other | Reference |
|---|---------------------|--------------|----------------|------------|--------------------------|
| | Once Through | Pond Cooling | Cooling Towers | | |
| Coal | | | | | |
| Fuel Production | | | | 0.26 | Gleick (1994) |
| Plant Operation | 0.3 | 0.3–0.48 | 0.48 | | Goldstein & Smith (2002) |
| Plant Operation | | | 0.68 | | NETL (2007) |
| Plant Operation | 0.32 | | 0.69 | | Gleick (1994) |
| Plant Operation | | | 1.2 | | NETL (2005) |
| Plant Operation | 0.064–0.14 | 0.004–0.8 | 0.46 | | NETL (2008) |
| Coal with Carbon Capture | | | | | |
| Fuel Production | | | | 0.01–0.17 | Harto et al. (2010) |
| Plant Construction | | | | 0.13–0.25 | Harto et al. (2010) |
| Plant Operation | | | | 0.5–1.2 | Harto et al. (2010) |
| Total Life Cycle | | | | 0.57–1.53 | Harto et al. (2010) |
| Nuclear | | | | | |
| Fuel Production | | | | 0.14 | Gleick (1994) |
| Plant Operation | 0.4 | 0.4–0.72 | 0.72 | | Goldstein & Smith (2002) |
| Plant Operation | | | 0.85 | | Gleick (1994) |
| Plant Operation | 0.14 | | 0.62 | | NETL (2008) |
| Natural Gas Conventional | | | | | |
| Fuel Production | | | | 0.29 | Gleick (1994) |
| Plant Operation | 0.3 | 0.3–0.48 | 0.48 | | Goldstein & Smith (2002) |
| Plant Operation | 0.29 | | 0.69 | | Gleick (1994) |
| Plant Operation | 0.09 | 0.11 | 0.16 | | NETL (2008) |
| Natural Gas Combined Cycle | | | | | |
| Fuel Production | | | | 0.22 | Gleick (1994) |
| Plant Operation | 0.1 | | 0.18 | | Goldstein & Smith (2002) |
| Plant Operation | | | 0.27 | | NETL (2007) |
| Plant Operation | | | 0.5 | | NETL (2005) |
| Plant Operation | | | 0.32 | | CEC (2006) |
| Hydroelectric | | | | | |
| Dam | 4.5 | | | | Gleick (1992) |
| Solar Thermal (Concentrated Solar Power) | | | | | |
| Plant Construction | | | | 0.02–0.08 | Harto et al. (2010) |
| Plant Operation | | | | 0.77–0.92 | Harto et al. (2010) |
| Total Life Cycle | | | | 0.87–1.12 | Harto et al. (2010) |
| Solar Photovoltaic | | | | | |
| Plant Construction | | | | 0.06–0.15 | Harto et al. (2010) |
| Plant Operation | | | | 0.006–0.02 | Harto et al. (2010) |
| Total Life Cycle | | | | 0.07–0.19 | Harto et al. (2010) |

| Life Cycle Stage | Cooling System Type | | | Other | Reference |
|---|---------------------|--------------|----------------|-----------|--------------------------------|
| | Once Through | Pond Cooling | Cooling Towers | | |
| Wind Onshore | | | | | |
| Plant Construction | | | | 0.02 | Vestas Wind Systems A/V (2006) |
| Plant Operation | | | | 3.62E-08 | Vestas Wind Systems A/V (2006) |
| Total Life Cycle ^a | | | | 0.01 | Vestas Wind Systems A/V (2006) |
| Geothermal — EGS | | | | | |
| Plant Construction | | | | 0.01 | Argonne |
| Plant Construction | | | | 0.36 | Frick et al. (2010) |
| Plant Operation | | | | 0.29–0.72 | Argonne |
| Plant Operation | | | 0.08 | | Frick et al. (2010) |
| Geothermal — Binary^{eb} | | | | | |
| Plant Construction | | | | 0.001 | Argonne |
| Plant Operation | | | | 0.27 | Argonne |
| Plant Operation | 0.15 | | | | Adee & Moore (2010) |
| Geothermal — Flash^{eb} | | | | | |
| Plant Construction | | | | 0.001 | Argonne |
| Plant Operation | | | | 0.005 | Argonne |
| Plant Operation | | | 0.01 | | Adee & Moore (2010) |
| Biomass | | | | | |
| Plant Operation | 0.3 | 0.3–0.48 | 0.48 | | Goldstein & Smith (2002) |
| Plant Operation | | | 0.61 | | Gleick (1994) |

^a Assumes recovery of water in the end-of-life management stage.

^{eb} Assumes water consumed as makeup for operational loss is a small percentage of total operational geofluid loss.

APPENDIX C – ADDITIONAL GEOCHEMICAL COMPOSITION DATA

This appendix contains additional geochemical data. Table C-1 contains the average and median concentrations as well as the total number of samples within the dataset for each chemical constituent for three different temperature ranges: the USGS “high” range of >150°C, the USGS “moderate” range of 90°C to 150°C, and all of the data in the dataset, including records without the temperature specified. Figures C-1 through C-8 profile the chemical compositions of geofluids from selected wells. The wells are identified by the name it is given in the dataset, the state where it is located, and the temperature of the sample.

TABLE C-1 Summary of Geofluid Constituent Concentrations for Different Temperature Ranges

| Constituent | High Temp (>150°C) | | | Moderate Temp (90°C – 150°C) | | | All Data | | |
|---------------------|--------------------|--------|---------|------------------------------|--------|---------|----------|--------|---------|
| | Mean | Median | Samples | Mean | Median | Samples | Mean | Median | Samples |
| Ag | 0.974 | 0.060 | 39 | 0.027 | 0.020 | 49 | 0.143 | 0.003 | 412 |
| Al | 73.2 | 1.00 | 78 | 13.9 | 0.223 | 132 | 11.9 | 0.020 | 1,887 |
| As | 2.19 | 0.490 | 171 | 0.716 | 0.040 | 833 | 0.729 | 0.011 | 8,322 |
| Au | 0.576 | 0.500 | 24 | 0.093 | 0.100 | 20 | 0.170 | 0.100 | 197 |
| B | 62.5 | 25.0 | 377 | 23.1 | 4.70 | 1,208 | 9.84 | 0.330 | 16,497 |
| Ba | 173 | 4.30 | 84 | 3.36 | 0.100 | 163 | 6.08 | 0.061 | 3,973 |
| Be | 0.013 | 0.002 | 26 | 0.018 | 0.002 | 52 | 0.014 | 0.002 | 323 |
| Bi | 1.44 | 0.250 | 8 | 0.066 | 0.066 | 1 | 0.248 | 0.026 | 61 |
| Br | 7.72 | 1.30 | 130 | 180 | 0.490 | 159 | 12.4 | 0.200 | 3,480 |
| Ca | 4,046 | 22.0 | 439 | 306 | 29.0 | 1,123 | 208 | 51.0 | 25,630 |
| Cd | 1.63 | 0.035 | 46 | 0.008 | 0.005 | 90 | 0.093 | 0.005 | 988 |
| Cl | 13,259 | 166 | 584 | 2,419 | 477 | 1,760 | 2,803 | 43.0 | 31,205 |
| Co | 0.130 | 0.010 | 38 | 0.027 | 0.030 | 78 | 0.093 | 0.010 | 957 |
| CO ₃ | 130 | 5.00 | 53 | 36.1 | 9.80 | 228 | 65.3 | 0.000 | 1,719 |
| Cr | 1.03 | 0.030 | 67 | 0.012 | 0.006 | 55 | 0.067 | 0.004 | 1,812 |
| Cs | 18.3 | 13.0 | 37 | 0.299 | 0.200 | 110 | 0.958 | 0.100 | 996 |
| Cu | 6.27 | 0.300 | 75 | 0.045 | 0.010 | 161 | 0.433 | 0.004 | 2,869 |
| F | 4.13 | 2.50 | 345 | 4.98 | 2.39 | 984 | 1.77 | 0.500 | 20,692 |
| Fe | 509 | 0.225 | 156 | 3.81 | 0.030 | 405 | 15.5 | 0.030 | 9,662 |
| Ga | 2.000 | 2.00 | 1 | 0.006 | 0.006 | 3 | 0.032 | 0.005 | 144 |
| Ge | 1.080 | 0.100 | 5 | 0.008 | 0.008 | 2 | 0.080 | 0.010 | 128 |
| H ₂ S | 6.40 | 5.90 | 54 | 4.51 | 1.83 | 98 | 9.06 | 1.000 | 805 |
| HCO ₃ | 313 | 262 | 240 | 246 | 201 | 483 | 300 | 222 | 5,570 |
| Hg | 0.192 | 0.005 | 73 | 0.005 | 0.0004 | 160 | 0.017 | 0.0002 | 1,284 |
| I | 3.78 | 0.500 | 44 | 0.808 | 0.040 | 90 | 1.65 | 0.030 | 1,128 |
| K | 2,477 | 53.0 | 420 | 121 | 13.3 | 1,091 | 147 | 5.00 | 22,516 |
| Li | 44.0 | 6.20 | 305 | 7.55 | 1.60 | 507 | 8.25 | 0.200 | 5,928 |
| Mg | 53.1 | 1.20 | 420 | 54.5 | 2.40 | 1,077 | 70.3 | 16.0 | 25,053 |
| Mn | 467 | 0.050 | 142 | 6.59 | 0.020 | 323 | 13.7 | 0.020 | 7,158 |
| Mo | 0.602 | 0.100 | 43 | 0.111 | 0.020 | 51 | 0.216 | 0.010 | 1,494 |
| Na | 8,625 | 612 | 423 | 1,791 | 231 | 1,122 | 1,605 | 57.0 | 24,778 |
| NH ₄ (N) | 271 | 245 | 43 | 24.7 | 0.500 | 96 | 53.7 | 1.51 | 665 |
| Ni | 28.7 | 0.100 | 46 | 0.142 | 0.030 | 72 | 1.65 | 0.013 | 1,271 |

TABLE C-1 (Cont.)

| Constituent | High Temp (>150°C) | | | Moderate Temp (90°C – 150°C) | | | All Data | | |
|---------------------|--------------------|--------|---------|------------------------------|--------|---------|----------|--------|---------|
| | Mean | Median | Samples | Mean | Median | Samples | Mean | Median | Samples |
| NO ₃ (N) | 4.72 | 0.200 | 49 | 8.54 | 6.20 | 205 | 6.29 | 2.10 | 1,296 |
| Pb | 65.4 | 80.0 | 69 | 0.092 | 0.050 | 101 | 4.38 | 0.010 | 1,394 |
| PO ₄ (P) | 0.249 | 0.100 | 49 | 0.336 | 0.100 | 100 | 0.348 | 0.100 | 443 |
| Rb | 151 | 6.00 | 48 | 0.264 | 0.170 | 141 | 7.48 | 0.100 | 1,091 |
| S | 36.6 | 6.00 | 14 | 1.99 | 1.00 | 15 | 25.06 | 3.00 | 118 |
| Sb | 0.734 | 0.400 | 53 | 0.228 | 0.141 | 90 | 0.273 | 0.094 | 701 |
| Se | 0.790 | 0.055 | 46 | 0.015 | 0.001 | 60 | 0.029 | 0.002 | 1,833 |
| SiO ₂ | 171 | 107 | 302 | 114 | 66.5 | 762 | 51.8 | 32.8 | 22,403 |
| Sn | 2.71 | 0.200 | 9 | ND | ND | 0 | 7.69 | 0.200 | 21 |
| SO ₃ | ND | ND | 0 | ND | ND | 0 | 0.400 | 0.350 | 49 |
| SO ₄ | 156 | 108 | 436 | 173 | 72.0 | 1,471 | 326 | 58.0 | 27,870 |
| Sr | 220 | 1.51 | 108 | 76.7 | 0.375 | 174 | 16.2 | 0.347 | 3,660 |
| Th | ND | ND | 0 | 0.0003 | 0.0003 | 2 | 0.0004 | 0.0001 | 51 |
| Ti | 1.68 | 0.100 | 5 | 0.040 | 0.015 | 6 | 0.099 | 0.009 | 174 |
| Tl | 0.002 | 0.002 | 9 | 0.219 | 0.100 | 17 | 0.073 | 0.004 | 55 |
| U | 0.779 | 1.00 | 19 | 0.029 | 0.0004 | 7 | 0.158 | 0.002 | 177 |
| V | 0.046 | 0.008 | 21 | 0.061 | 0.010 | 44 | 0.037 | 0.009 | 1,027 |
| W | 0.680 | 0.100 | 5 | ND | ND | 0 | 0.144 | 0.028 | 48 |
| Zn | 250 | 0.073 | 82 | 0.228 | 0.021 | 207 | 6.48 | 0.020 | 4,373 |

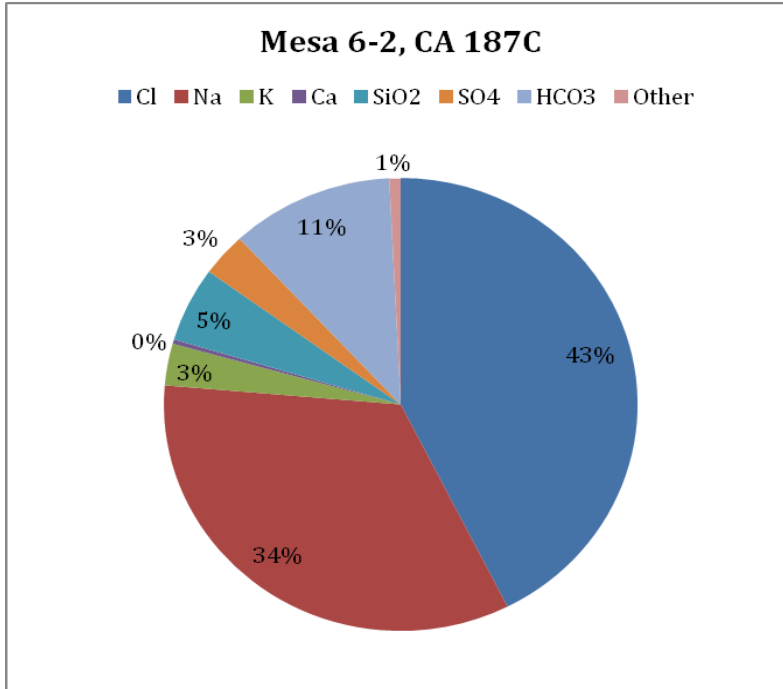


FIGURE C-1 Geofluid Composition, Sample from Mesa 6-2 Well in CA at 187°C

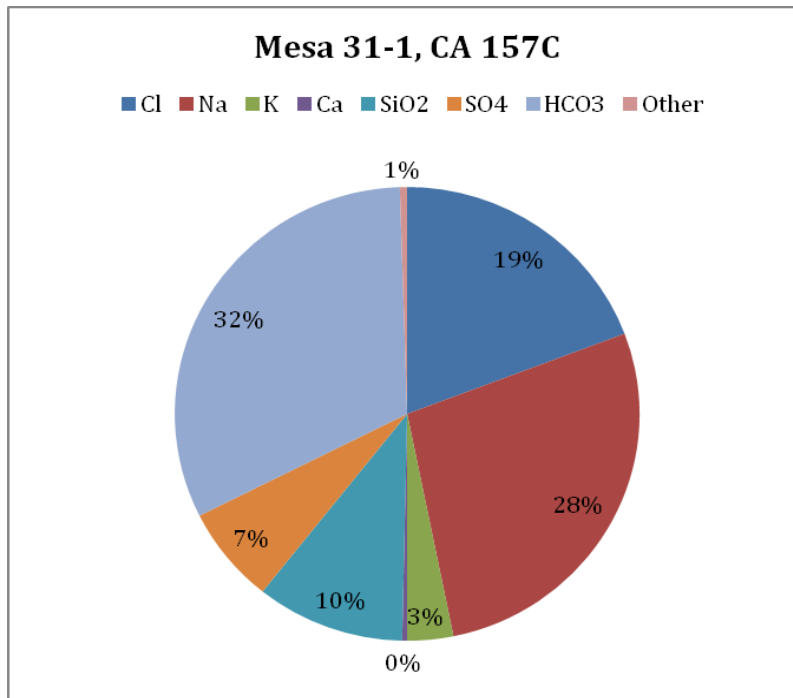


FIGURE C-2 Geofluid Composition, Sample from Mesa 31-1 Well in CA at 157°C

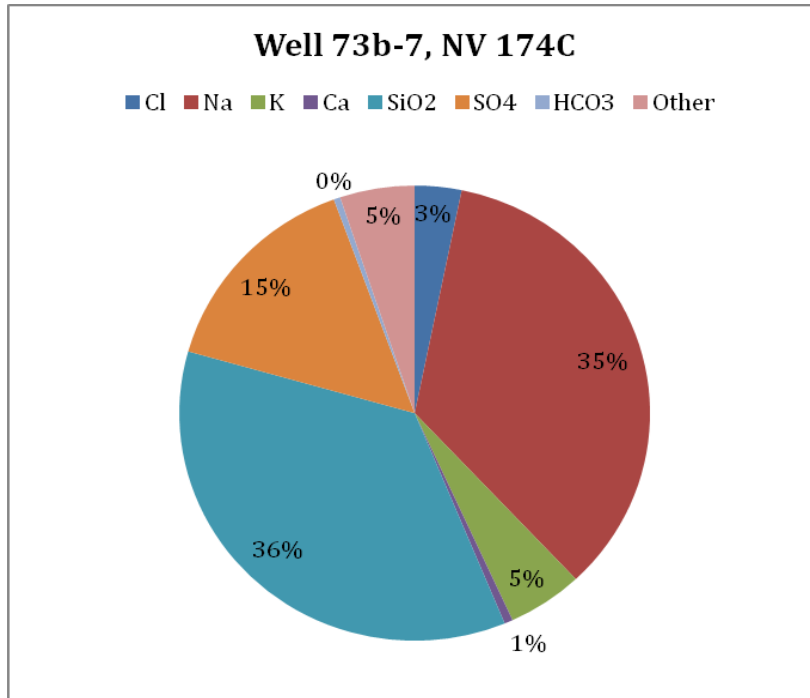


FIGURE C-3 Geofluid Composition, Sample from Well 73b-7 in NV at 174°C

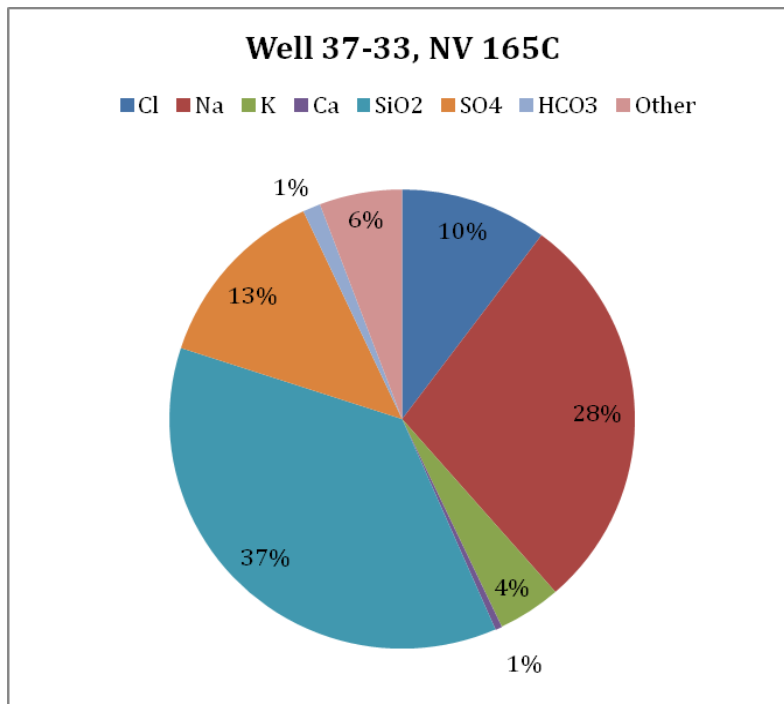


FIGURE C-4 Geofluid Composition, Sample from Well 37-33 in NV at 165°C

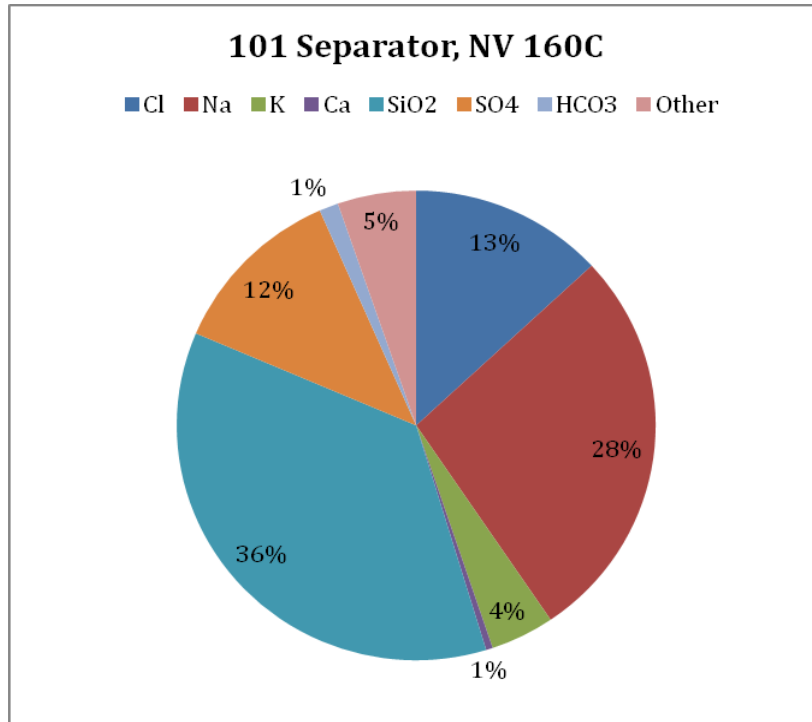


FIGURE C-5 Geofluid Composition, Sample from the 101 Separator in NV at 160°C

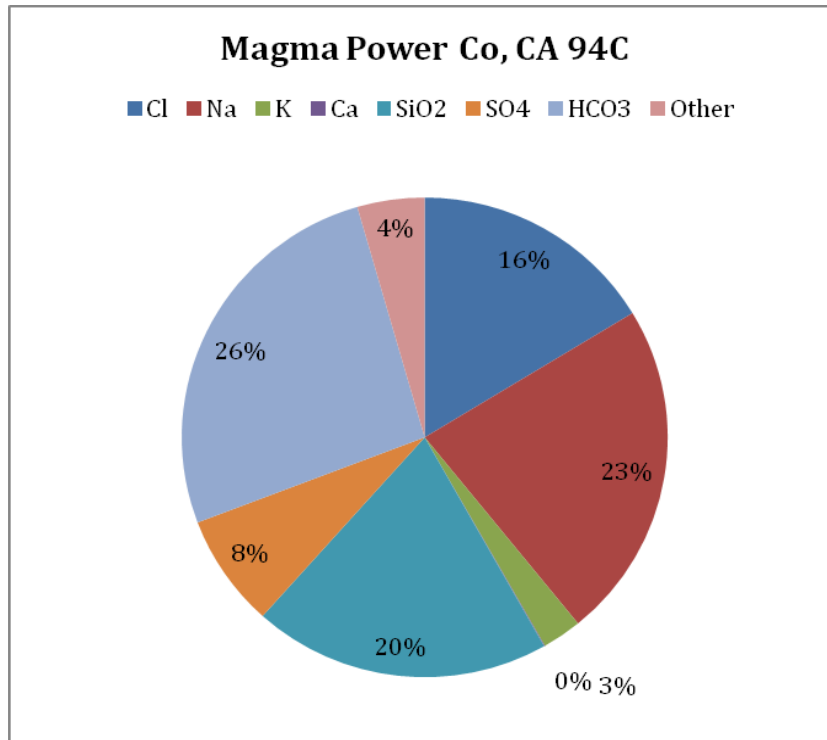


FIGURE C-6 Geofluid Composition, Sample from Magma Power Co., Unspecified well in CA at 94°C

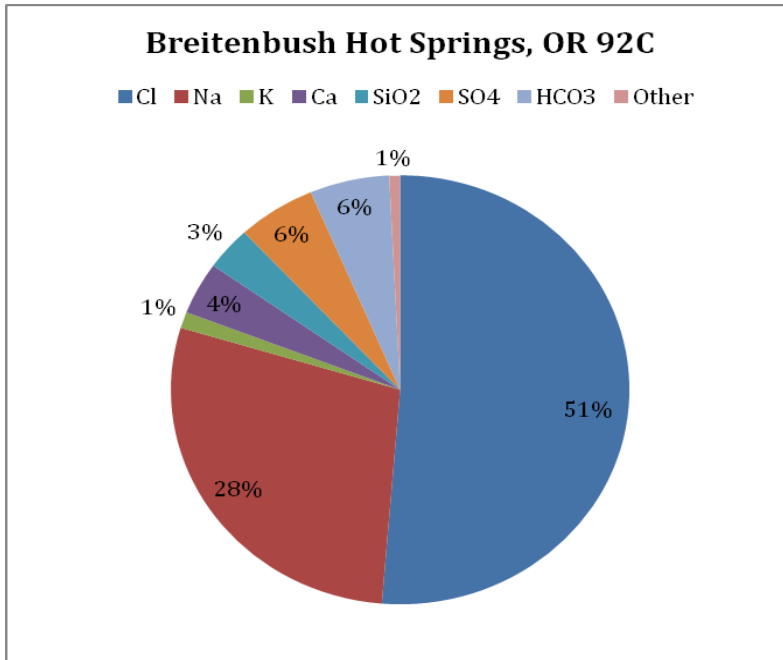


FIGURE C-7 Geofluid Composition, Sample from Breitenbush Hot Springs, in OR at 92°C

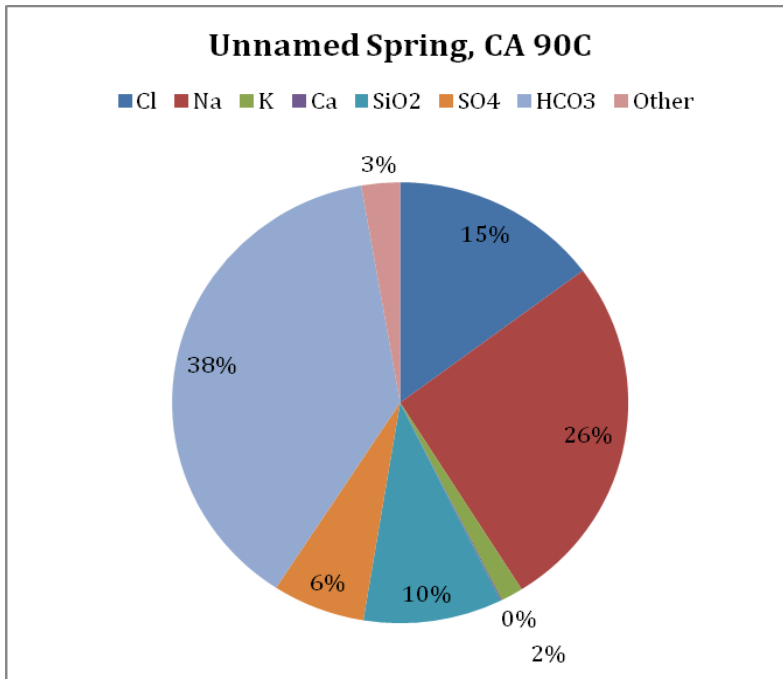


FIGURE C-8 Geofluid Composition, Sample from an Unnamed Spring in CA at 90°C

APPENDIX D – ADDITIONAL GAS COMPOSITION DATA

This appendix contains additional noncondensable gas (NCG) data. Figures D-1 through D-11 contain pie charts representing additional samples of NCG composition from various wells throughout the U.S.

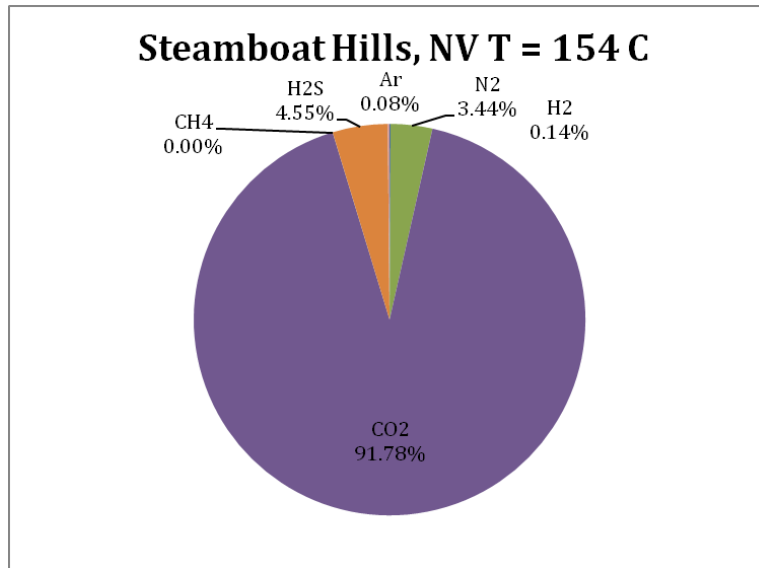


FIGURE D-1 NCG Composition, Sample from Steamboat Hills in NV at 154°C

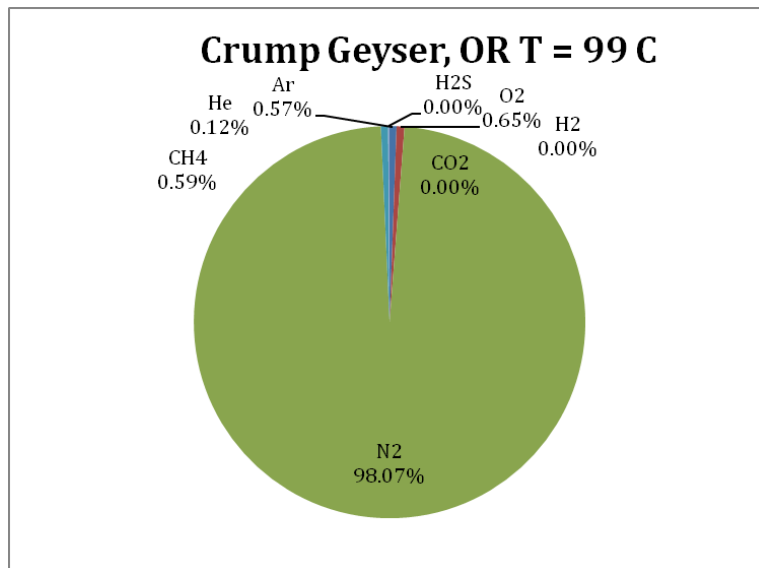


FIGURE D-2 NCG Composition, Sample from Crump Geyser in OR at 99°C

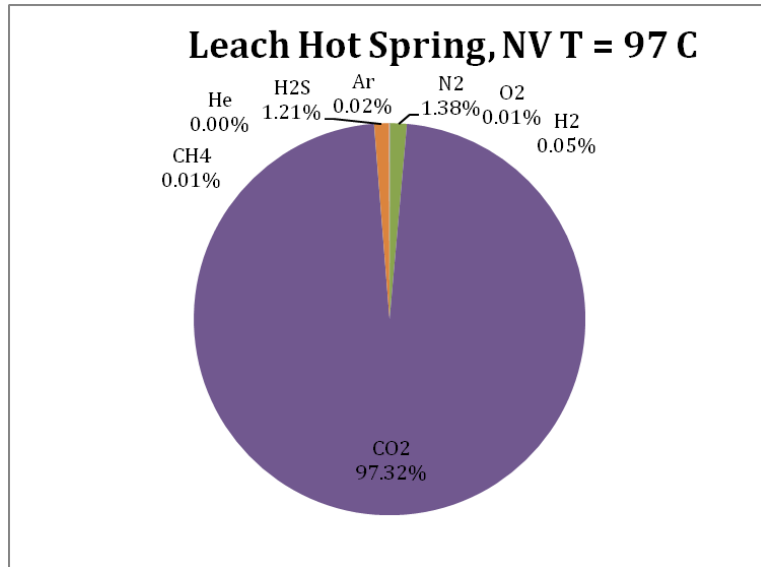


FIGURE D-3 NCG Composition, Sample from Leach Hot Spring in NV at 97°C

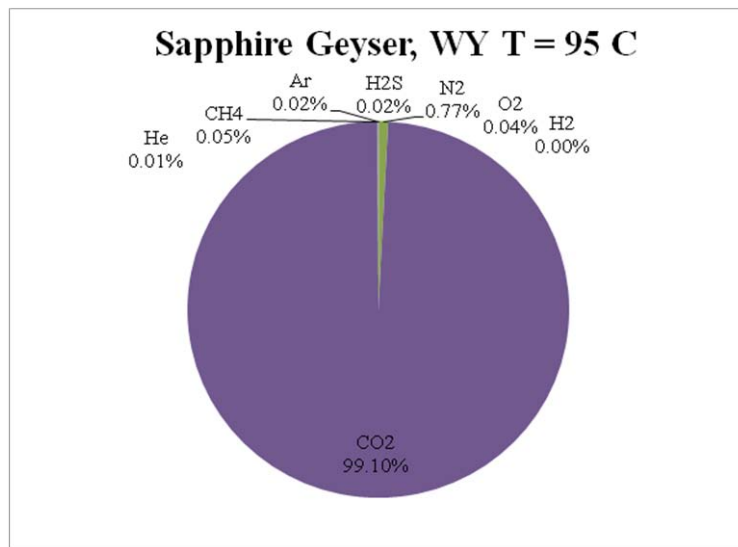


FIGURE D-4 NCG Composition, Sample from Sapphire Geyser in WY at 95°C

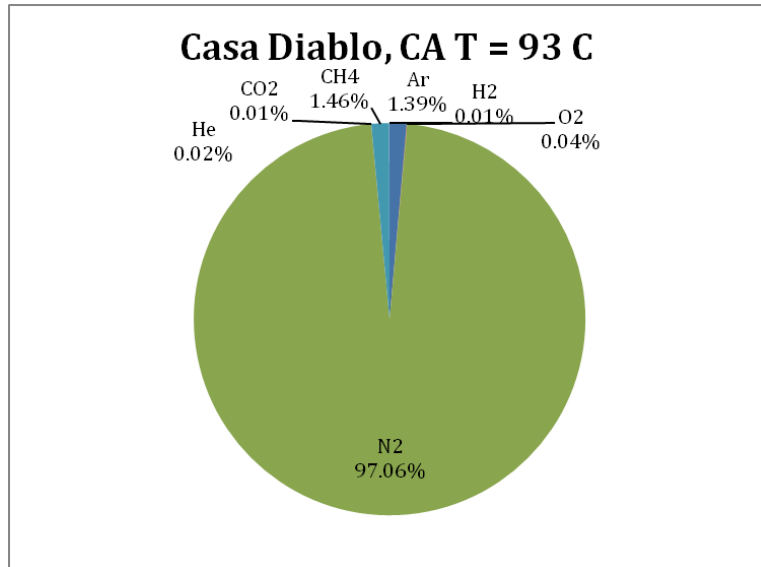


FIGURE D-5 NCG Composition, Sample from Casa Diablo in CA at 93°C

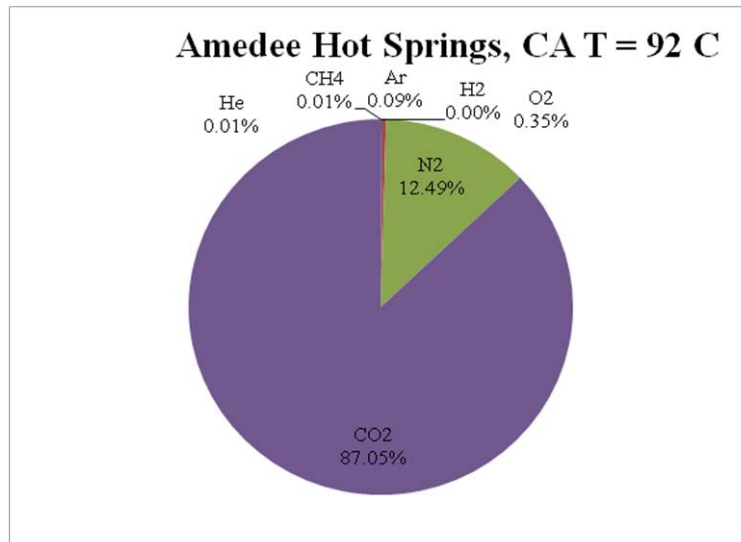


FIGURE D-6 NCG Composition, Sample from Amedee Hot Springs in CA at 92°C

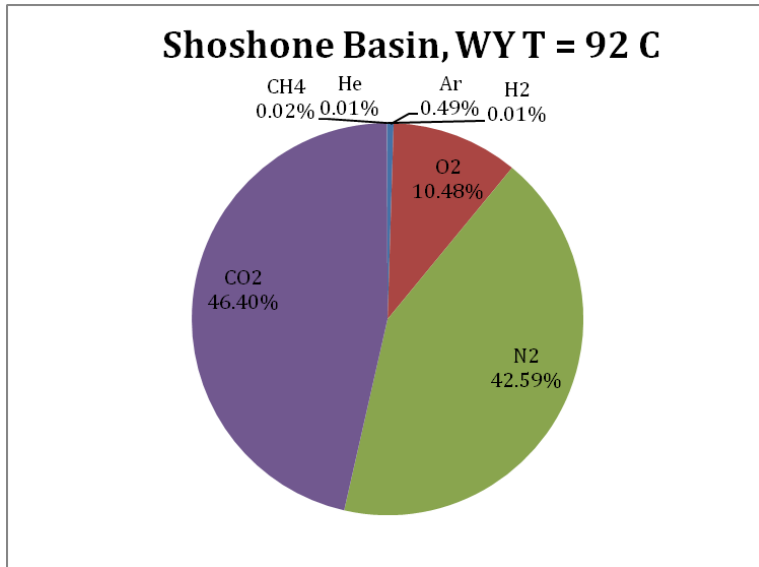


FIGURE D-7 NCG Composition, Sample from Shoshone Basin in WY at 92°C

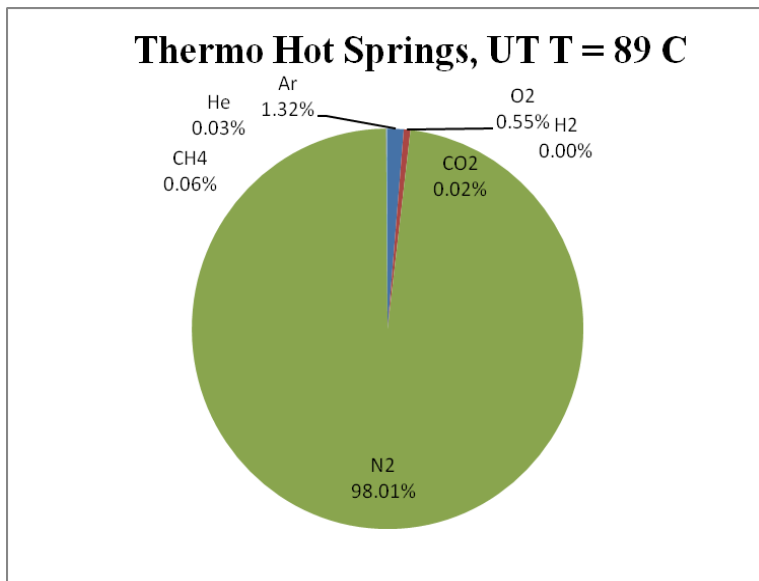


FIGURE D-8 NCG Composition, Sample from Thermo Hot Springs in UT at 89°C

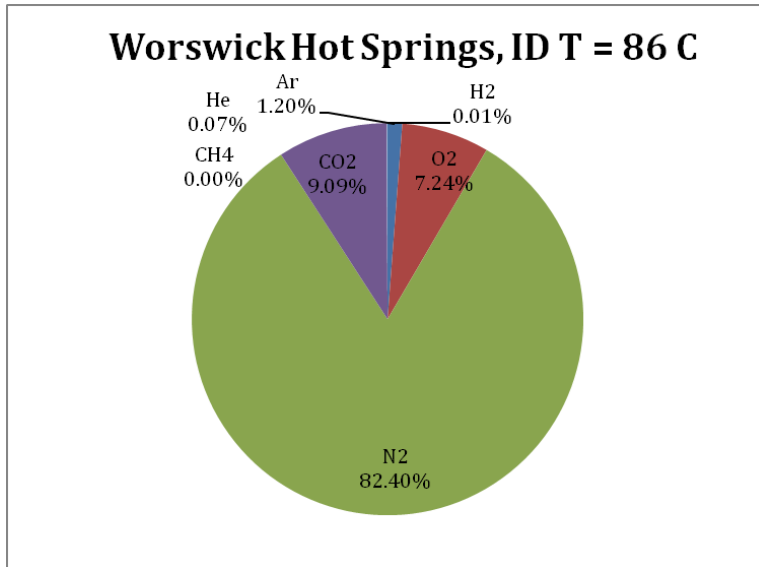


FIGURE D-9 NCG Composition, Sample from Worswick Hot Springs in ID at 86°C

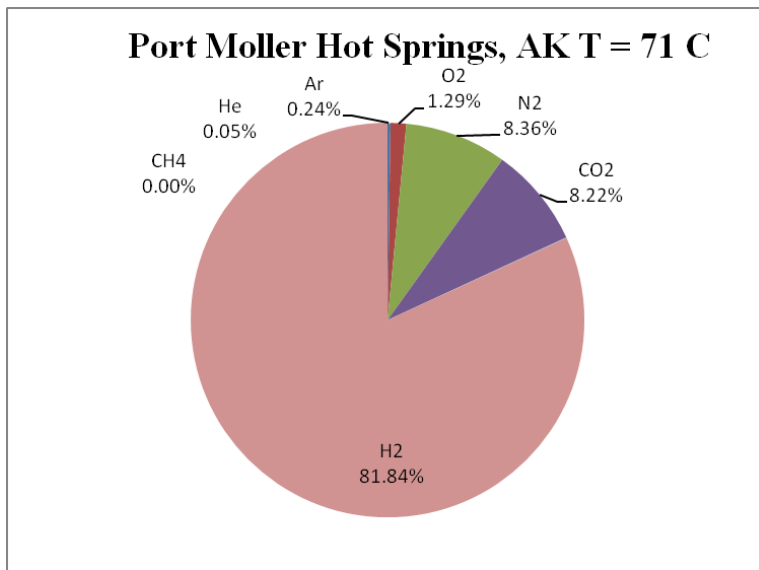


FIGURE D-10 NCG Composition, Sample from Port Moller Hot Springs in AK at 71°C

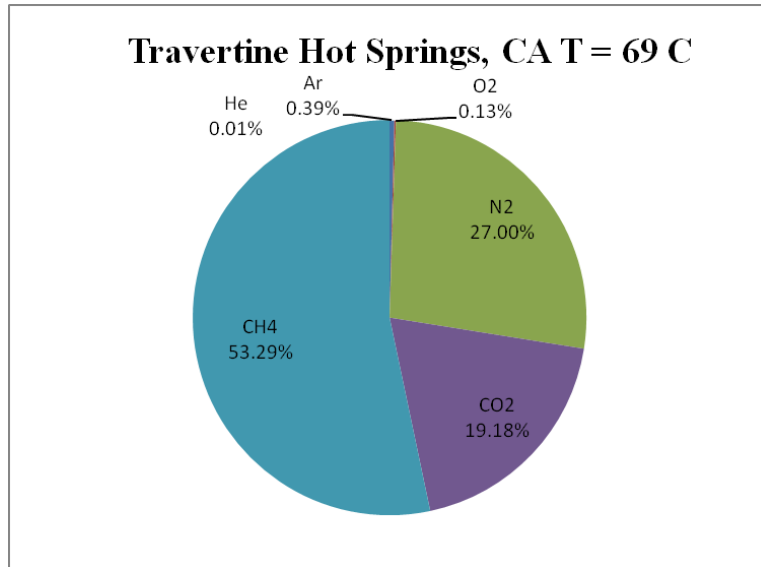


FIGURE D-11 NCG Composition, Sample from Travertine Hot Springs in CA at 69°C



Environmental Science Division

Argonne National Laboratory
9700 South Cass Avenue, Bldg. 240
Argonne, IL 60439-4847

www.anl.gov



**U.S. DEPARTMENT OF
ENERGY**

Argonne National Laboratory is a U.S. Department of Energy
laboratory managed by UChicago Argonne, LLC